CHAPTER 4

Phytochemical analysis of *Oreocnide integrifolia* extract and, *in-vitro* and *in-vivo* bioactivity assessment of selected fractions in terms of insulin secretion and glucose uptake

Introduction:-

Despite being one of the oldest diseases, a composite therapy has eluded the world to date for diabetes mellitus and, WHO has declared it as a chronic disease. It is proving to be a serious life threatening heterogeneous metabolic disorder affecting carbohydrate, lipid and protein metabolisms and afflicting nearly an estimated 191 million people in 2000 and expected to affect an estimated 306 million by 2030 (Moller and Filler, 1991; Wild *et al.,* 2004). The metabolic derangements characteristic of diabetes in general is due primarily to a complete or relative insufficiency of insulin secretion and / or insulin action (Balkan *et al.,* 2000). The escalated frequency of the disorder is likely to impact the population of developing countries due to expensive and inadequate treatments coupled with the lack of effective and affordable interventions (Djrolo *et al.,* 1998; Marx, 2002). Chronic hyperglycemia along with glucosuria, polydypsia, polyurea and ketoacidosis are symptomatic of diabetes and is by itself an independent risk factor for the prognosis of cardiovascular disorders and dyslipidemia.

Since the causes of diabetes are multifactorial and fraught with life threatening consequences, the disorder is in urgent need of a multimodal cost-effective therapeutic intervention that is more potent and sans side effects. It is in this context that the World Health Organisation (WHO) has encouraged and recommended the use

of herbs as an alternative therapy for diabetes (WHO, 1980) and, though a wide range of medicinal plants are in use world over, many of them are however with no valid scientific sanctity. The suggested need for alternative therapy has pinned renewed attention on the search for plant based anti-diabetic agents, also favoured due to their easy availability, effectiveness, affordability and probable low ill-effects (Marles and Farnsworth, 2005). Apparently, a systematic scientific scrutiny of the anti-diabetic potentials of these plants has become a matter of utmost importance to justify their application in ethnomedicine. Due to their rich diversity and complement of active phytochemicals and secondary metabolites, plants from ancient human civilization have been used as medicament for very many ailments (Fabricant and Farnsworth, 2001; Tapsell *et al.,* 2006; Dwivedi and Dwivedi, 2007; Acharya and Srivastava, 2008). Plants/ herbs constitute the main stay of health care system in rural areas due to limited access to modern health facilities.

Indian rural and folklore ethnomedical practices involve usage of many relatively unknown medicinal plants with scientifically non-characterised pharmacological activities. One such plant is "*Oreocnide integrifolia*" popular in north-eastern parts of India, especially Manipur, used as a folklore anti-diabetic therapeutant. In this context, a scientific evaluation of this plant was initiated by us on various animal models of type 1 and type 2 diabetes (Chapter 1-3). Having found favourable effects on glucoregulation, insulin sensitivity, redressal of deviant carbohydrate metabolism, peripheral glucose uptake, reversal of dyslipidemia etc., it was thought pertinent to carry out a phytochemical analysis of OI leaves by subjecting to various solvent extractions and qualitative analysis and, by further subjecting the active fraction to HPTLC finger printing.

Since the primary defects of diabetes are centred around β-cell dysfunction, insulin secretion and insulin action, it was thought desirable to test the bioactivity of whole leaf aqueous extract on isolated islets and of the various solvent extracts on RINm5F cell line for glucose stimulated insulin secretion and also on C2C12 cell line for basal or insulin induced glucose uptake. Further, it was envisaged to test the glucose stimulated insulin secretion and anti-oxidant property of the most active fraction (flavonoidal rich fraction) on streptozotocin exposed islets. Further, the dose dependent anti-diabetic potential of the active fraction has also been tested *in-vivo* using multidose streptozotocin exposed mice.

Materials and Methods:

1. **Phytochemical Analysis:**

Phytochemical Screening: Phytochemical tests were carried out for various constituents of OI leaf extract using the following chemicals and reagents. Dragendorff's reagent was used for alkaloids, frothing test for saponins, Liebermann–Burchard test for sterols, $FeCl_3$ for tannins, Molisch reagent for carbohydrates, ninhydrin for proteins and vanillin/sulfuric acid for terpenoids (Wagner *et al.*, 1994; Barbehenn, 1995; Cannell, 1998; Evans, 2002). Quantitative analyses of secondary metabolites were carried out for polyphenols (Hagerman *et al.*, 2000b), flavonoids (Chang *et al.*, 2002), tannins (Liao and Shi, 2005) and saponins (Xi *et al.*, 2007).

Extractions and Fractionation: Fresh green leaves were dried and powdered in a grinder. About 100gm of this powder was mixed with 500 ml of n hexane in stoppered round bottomed flask. After 48 hrs, the mixture was filtered and hexane was concentrated using rota evaporator (Buchi, Germany) and designated as hexane

fraction. The hexane fraction is usually known to consist of non-polar compounds like fatty acids, waxes, hydrocarbons, sterols, triterpenoids etc. The defatted powder was dried free from hexane and subjected to sequential solvent extraction using soxhlet apparatus with Chloroform, Ethyl acetate, Methanol and n-Butanol.

Flavonoid rich fraction: Briefly, One hundred gms of air-dried leaves were ground to fine powder and soaked in 70% ethanol for 24 h with continuous stirring. After soaking, the mixture was filtered with Whatmann No. 1 filter paper. The filtrate obtained was centrifuged at 10,000 rpm at room temperature (25°C) and the pellet was discarded. The supernatant was concentrated in vacuo by means of a rotavapor .The concentrated extract was then dissolved in as little water as possible and washed three times with chloroform. The residual layer was extracted three times with ethyl acetate. This fraction was concentrated in vacuo and designated as flavonoid rich fraction (FRF) and subsequently subjected to phytochemical analysis. The flavonoid rich fraction was then used for bioactivity assays *in vitro*.

GC-MS: Hexane extract was subjected to analysis of volatile and non-polar constituents. Gas chromatography coupled with mass spectrometry was carried out on Agilent 689ON Network GC system combined with Agilent 5973 network mass selective detector. The capillary column used was an Agilent 19091N-136 (HP innowax capillary, 60m X 0.25mm X 0.25μm).Helium was used as a carrier gas at a flow rate of 3.3ml/min with 1μl injection volume. Samples were analyzed with column initially at 100°C for 1 min after injection, then increased to 170°C with 10°C/min heating ramp without hold and increased to 215°C with 5°C/min heating ramp for 5 min. The final temperature was increased to 240°C with 10°C/min heating

ramp for 10 min. The injections were performed in split mode (30:1) at 250°C.Detector and injector temperature were 260°C and 250°C respectively. Pressure was established at 50 psi and the run time was 35 min. Temperature and nominal initial flow for flame ionization detector (FID) were set as 250°C and 1ml/min. Correspondingly, MS parameters were as follows: Scan range (m/z) 35-450 AMU under EI ionization (70ev). Identification of components was based on retention indices relative to n-alkanes and mass spectra matching NIST Wiley 275L library as well as by comparison of fragmentation pattern with published literature.

Isolation of non-polar compounds: Hexane extract (yield 34.76%) was chromatographed on a silica gel column (Merck 70-230 mesh, 1200 gms; 3cm internal diameter X 100 cm) and successively eluted with a step wise gradient of Hexane, hexane and ethyl acetate, ethyl acetate and methanol and finally methanol. The fractions were collected and each fraction was spotted on a precoated Silica gel 60 F_{254}, 0.25-mm-thick TLC plate (Merck) and fractions with similar R_f values in TLC pattern were pooled together. Pure compounds were submitted for spectroscopic analysis.

HPTLC fingerprint of Methanolic extract /flavonoidal rich fraction: TLC finger print profile was established for methanolic extract using HPTLC. A stock solution (1 mg/ml) of methanolic extract was prepared in methanol. A Camag HPTLC system equipped with an automatic TLC sampler (ATS 4), TLC scanner 3 integrated with software (WinCATS version 1.4.2) and UV cabinet and automatic developing chamber ADC2 with humidity control facility was used for the analysis. The samples

were applied using automated TLC sampler in 10 mm bands, 10 mm from the bottom and 15 mm from the sides, with 8 mm space between the two bands. Plates were developed in software controlled Camag automatic developing chamber ADC2 pre-saturated with 10 ml of developing solvent phase for 30 min at room temperature (25°C) and, relative humidity was maintained (45%). The plates were developed to a height of about 8 cm from the base in Chloroform: Methanol; 95:5 (v/v) and Ethyl acetate: Formic acid: Glacial acetic acid: Water; 100:11:11:26 (v/v). After development, the plate was removed, dried and, spots were visualized under UV light (254; absorbance/reflectance mode or 366 nm; fluorescence / reflectance mode) and Rf values, spectra, λ_{max} and, peak areas of resolved bands were recorded. Spray reagents like Dragendorf's, Nitroblue tetrazolium, and Anisaldehyde-sulphuric acid were used to detect different classes of compounds.

High Pressure Liquid Chromatography (HPLC)

Chromatography was performed on Shimadzu (Shimadzu Corporation, Kyoto, Japan) chromatographic system equipped with Shimadzu LC-20AT pump and Shimadzu SPD-20AV absorbance detector. Samples were injected through a Rheodyne 7725 injector valve with fixed loop at 20 µL. Data acquisition and integration were performed using Spinchrome software (Spincho biotech, Vadodara). HPLC grade acetonitrile (ACN) and methanol (Spectrochem Ltd, Mumbai), analytical grade Ammonium acetate (Merck, India) and purified water from Millipore Milli-Q system were used for the experiment. For qualitative analysis, about 20mg sample (flavonoid rich fraction) was dissolved in methanol and filtered through a 0.22µm Millipore membrane filter. All standards were dissolved in methanol except for Hesperidin which was dissolved in DMF.

Chromatographic condition

Condition I:

HPLC separation of morin, rutin, apigenin and quercetin along with flavonoidal rich fraction was performed at room temperature on a Reverse phase C18 (250mm X 4.6mm i.d., 5µm particle size) column with mobile phase composed of 0.5% v/v phosphoric acid: methanol (50:50). The flow rate was set to 1.0 mL/min and UV detection was carried out at 254 nm. An injection volume of 20 µL was used. Mobile phase/solvent blank run was performed for all analysis.

Condition II:

HPLC separation of kaempherol, hesperidin, naringin, quercetin and rutin along with flavonoidal rich fraction was performed at 40°C on a Reverse phase C18 (250mm X 4.6mm i.d., 5µm particle size) column with mobile phase composed of 5mM ammonium acetate (pH 4.45 adjusted with acetic acid) : acetonitrile (75: 25). The flow rate was set to 1.0 mL/min and UV detection was carried out at 254 nm. An injection volume of 20 µL was used.

2. *In vitro* and *in vivo* bioactivity assays:-

Mouse Islet Isolation: Islet isolation was performed according to the methods of Lacy and Kostianovsky (1967) and Shewade et al. (1999). Groups of three BALB/c mice were killed by cervical dislocation, and splenic pancreas was removed under sterile conditions without ductal injection and distention. Briefly, the pancreas was cut into small pieces/chopped finely ~1mm^2 and was subjected to enzymatic digestion for 10–12 min by vigorous mechanical shaking in a water bath maintained at 37°C. The dissociation medium consisted of Dulbecco's Modified Minimum Essential Medium

(DMEM) supplemented with Collagenase type V (1mg/ml; Sigma, St. Louis, MO), and 2% BSA fraction V (Hi-Media Labs, Mumbai). The tissue digested was then centrifuged at 1500g for 10 min, washed twice in PBS (pH: 7.4) and seeded in culture flasks (25 cm^2; Nunc, Denmark) containing RPMI-1640 (Hyclone, USA) supplemented with 10% (v/v) FBS (Hi-Media, India), 100U/ml penicillin and 100U/ml streptomycin under 95% O_2 and 5% CO_2 atmosphere at 37°C (Thermo, USA) in air. Under these culture conditions, most of the acinar cells degenerate within 48 hrs leaving behind islets. After 48 hrs of incubation, islets were separated from exocrine pancreas by hand-picking using a binocular stereomicroscope and quantified using automated Microsoft Excel sheet ; wherein number of islet equivalents was counted on the basis of their size. For further purification, islets (removal of acinar cells) were isolated using density gradient Ficoll reagent- Type 400 (Hi-Media Labs, Mumbai) present in 20-11% interface. The islets were specificity assessed using dithizone staining (Hi-Media, Mumbai, Maharashtra, India) while islet viability was assessed using Trypan blue staining.

Glucose induced insulin secretion assay: Isolated islets were cultured at 37°C in a humidified atmosphere of 5% CO_2 in air in RPMI-1640 medium containing 10% FBS and antibiotics. Islets were seeded at a concentration of 100 or 50 islets per well in 24-well plates (Falcon, NJ) and allowed to attach overnight prior to acute tests. Wells were washed three times with Krebs–Ringer bicarbonate buffer (KRB; 115 mM NaCl, 4.7 mM KCl; 1.3 mM $CaCl_2$, 1.2 mM KH_2PO_4, 1.2 mM $MgSO_4$, 24 mM $NaHCO_3$, 10 mM HEPES, 1 g/L BSA, 1.1 mM glucose; pH 7.4) and preincubated for 1 hr at 37°C. Unless otherwise stated, wells were then incubated for 1 h in 1 ml KRB with 4.5 mM or 16.7 mM glucose and OI extract/FRF (10, 50, 100 or 250μg/ml). Aliquots were

removed from each well, centrifuged (2000 rpm for 5 min, at 4°C), and assayed for insulin using mouse insulin ELISA kit and protein concentration was determined.

Cell lines: RINm5F and C2C12 cell lines were procured from National Centre for Cell Sciences, Pune, India. The RINm5F cells were maintained in RPMI 1640 supplemented with 10% FCS, 100IU penicillin/ml and 100 µg streptomycin/ml and incubated at 37 °C under a humidified 5% CO_2 atmosphere. The cells were grown in 25 cm^2 tissue culture flasks until confluence and then sub-cultured for experimentation. Glucose stimulated insulin secretion (GSIS) assay was performed on RINm5F cell line as previously described.

2NBDG glucose uptake: The C2C12 skeletal muscle cell line was maintained in Dulbecco's Modified Eagle Medium (DMEM) supplemented with 15% Foetal Calf Serum and antibiotics (Penicillin 100IU/ml and Streptomycin 100µg/ml) in 5% CO^2 at 37°C.After attainment of ~70% confluency, the cells were switched to 2% horse serum for 3 days for differentiation. The differentiated myotubes were seeded in 96 well fluorescence plates with BSA (1mg/ml) and 80µM fluorescent analogue; 2-[*N*-(7-Nitrobenz-2-oxa-1,3-diazol-4-yl) amino]- 2-deoxy-d-glucose [2NBDG , Invitrogen, Carlsbad, CA] in presence of different concentrations of various fractions or FRF for 60 min. For stimulation experiments 100nM insulin was added along with fractions or FRF. The cells were washed three times to remove free 2NBDG and, plates were read at excitation wavelength of 485nm and an emission wavelength of 535nmn using Fluorescent micro plate readers (Molecular Devices, Sunnyvale, USA).

Dose optimization (islet studies): Optimization for different concentrations/ doses of STZ (1mM, 2mM and 5mM) and for duration of STZ exposure (2hr, 6hr, 8hr and 12hr) was done. Different concentrations of FRF (10, 50, 100 and 250 µg/ml) were used for STZ insult/stress experiments. 2mM STZ with an exposure time of 8 hr was characterised as the best optimized schedule for experimental studies. Experimental groups consisted of Control and STZ treated islets that were pretreated with FRF for a period of 24 hr.

MTT assay: The viability of cultured islets was determined by assaying the reduction of 3-(4, 5-dimethylthiazol-2-yl)- 2, 5-diphenyltetrazolium bromide (MTT) to formazan. Briefly, islets were seeded in 24-well microtiter plates (50 islets per well) and left overnight to adhere before being exposed to different concentrations of STZ and FRF. In each experiment, different concentrations of FRF (10, 50, 100, 250 µg/ml) along with 2mM STZ were tested in three separate wells and the cytotoxicity assessed from at least three different experiments. After exposure to STZ and FRF, 50µl of 5mM MTT solution was added to each well, and incubated in the dark at 37°C for 4 h. Thereafter, MTT was removed and the formazan crystals were dissolved in 200 µl of DMSO. The absorbance was measured at 570 nm using a Microplate Reader (Biotek, USA).

DCF-DA measurements: The intracellular formation of reactive oxygen species was measured using 2′, 7′-dichlorodihydrofluorescin diacetate (DCFH-DA) (Sigma-Aldrich, MO, USA). The non-fluorescent compound DCFH-DA penetrates into the cell and is cleaved by intracellular easterases, resulting in the formation of 2′, 7′-dichlorodihydrofluorescin (DCFH), the oxidation of which (due to oxidative stress)

generates the fluorescent compound dichlorofluorescein. Thus, the DCF fluorescence represents the rate and quantity of ROS produced. Fifty islets from all treatment groups were incubated in fresh media and incubated with 10 μM DCFH-DA at 37°C for 30 min, washed twice with PBS and the fluorescence measured using a fluorimeter (Hitachi 6300, Japan) with excitation at 495 nm and emission at 538 nm. All values were corrected by subtracting auto fluorescence for respective wells. The results were expressed as relative fluorescence units/50 islet equivalents.

Intracellular Calcium levels: The intracellular calcium concentration, $[Ca^{2+}]i$, was measured using fura-2AM (Molecular Probes, Invitrogen, USA). Fura-2AM crosses cell membranes and once inside the cell, the acetoxymethyl groups are removed by cellular esterases to generate fura-2, the fluorescent calcium indicator. Islets were incubated in calcium free HBSS with 5μM fura-2AM at 37°C for 30 min in shaking water bath. After washing (2×) with calcium free HBSS, islets were suspended in complete HBSS and treated with various concentrations of FRF for 60 min in a shaking water bath. Fluorescence was measured with spectrofluorometer (Hitachi 7000, Japan) at an emission wavelength of 500nm for dual excitation wavelength at 340 and 380nm. The $[Ca^{2+}]i$ was expressed as nmole/50 islet equivalents.

cAMP measurements: For cAMP measurements, islets cultured in 24-well plates were exposed to 11.1 mM glucose for 60 min in the presence of the phosphodiesterase inhibitor 3-isobutyl-1-methylxanthine (1 mM) [IBMX] and various concentrations of FRF. At the end of incubation, islets were lysed following the manufacturer's instructions, and cAMP quantification was performed using a cAMP direct

immunoassay kit (Abcam, USA) and normalized to protein concentrations. Results were expressed as fmol/μg protein.

Peroxynitrite measurements: Concentration of peroxynitrite from respective treatment groups was estimated by incubating 50 islets with 10 μM dihydrorhodamine 123 (DHR123) for 30 min. Fluorescence was measured using excitation at 500 nm and emission at 530 nm (Hitachi 7000 Spectrofluorimeter). Auto-fluorescence was deducted from total fluorescent count for corrected fluorescent intensity and was expressed as relative fluorescence units/50 islets equivalents.

Nitric oxide measurements: Concentration of Nitric oxide from respective treatment groups was estimated by incubating 50 islets with fluorescent probe DAF-FM (1μM) for 30 min and then washed with PBS. Fluorescence was measured using excitation at 485 nm and emission at 520 nm (Hitachi 7000 Spectrofluorimeter). Auto-fluorescence was deducted from total fluorescent count for corrected fluorescent intensity and was expressed as relative fluorescence units/50 islets equivalents.

MMP measurements (Rhodamine 123): Mitochondria are vulnerable targets for various toxicants because of their important role in maintaining cellular integrity and functions. Functional alterations occur in mitochondria due to changes in mitochondrial membrane potential. Disruption of the mitochondrial membrane potential (i.e. depolarization) is one of the earliest indicators of cellular disturbance. Fifty islets were loaded with a cationic fluorescent dye Rh-123. From the respective treatment groups, islets were changed to serum free medium containing Rh-123

(10μM) and incubated for 30 min at 37°C. Results were expressed as relative fluorescent units/50 islet equivalents.

LPO measurements: Lipid peroxidation was measured in terms of micro moles of malondialdehydes formed. Briefly, islets were suspended in 200μl of 1.15% KCl. To this suspension 0.8% TBA, 1% SDS and 20% acetic acid were added. The reaction mixture was kept at 90°C for 45 min and immediately cooled on ice. The pink colour representative of thiobarbituric acid reactive substances was measured at 532 nm and protein concentration determined. The values were expressed as nmoles of MDA formed/mg protein.

Multiple dose Streptozotocin model: For induction of diabetes, BALB/c mice (30-35gm) were fasted overnight and injected with 50mg/kg body weight of streptozotocin dissolved in sodium citrate buffer (pH 4.5) intraperitoneally for five consecutive days. Mice were provided 10% sucrose solution to prevent sudden hypoglycemia. Mice that exhibited frank diabetes (blood glucose levels > 200mg/dl after 4 weeks) were considered for the experimental studies.

Glucose and insulin: Blood glucose was measured using Glucometer (Roche Diagnostics, US) and insulin levels were measured using mouse insulin ELISA (Crystal Chem, USA) with an intra-assay of coefficient variance of > 5%.

Terminal dUTP transeferase mediated Nick-End Labelling (TUNEL) Assay:

TUNEL assay was performed to assess the *In Situ* DNA fragmentation in control and experimental animals. The TUNEL assay was performed in paraffin embedded pancreas sections according to the manufacturer's instructions using APO-BrdU™ TUNEL Assay Kit (Invitrogen, USA). Breifly, after the treatment period, the animals were sacrificed and pancreas were excised and preserved in 4% w/v paraformaldehyde in buffered saline solution (1-2 drops of 1M NaOH in PBS).The tissues were washed thoroughly in repeated changes of 70% alcohol and then dehydrated in ascending grades of alcohol (70-100%). After dehydration, the tissues were cleared in toluene and embedded in paraffin wax. Sections of 5µm thickness were cut on a rotary microtome (Leica, Germany) and taken on glass slides coated with Poly-L-Lysine (Sigma Aldrich, USA). Sections were deparaffinated in fresh xylene followed by alcohol grades (100, 95, 85, 70 and 50%) and washed with PBS. Fixation was done using fresh 4% paraformaldehyde (PFD) followed by Proteinase K treatment (20 µg/ml of Proteinase K Solution was prepared combining 2 µl of 10 mg/ml Protease K and 998 µl of 100 mM Tris-HCl, pH 8.0, 50 mM EDTA). Slides were again fixed in 4% PFD and washed with PBS. Sections were marked with PAP Pen (Invitrogen USA) and covered with Wash buffer. Slides were gently tapped to remove excess liquid and 50 µl of the DNA Labeling Solution (Mix 10 µl of reaction buffer, 0.75 µl of TdT enzyme, 8.0 µL of BrdUTP and 31.25 µL of dH_2O) per section was gently placed on the slides in dark humidified chamber. After incubation, the slides were rinsed with PBS for 5 min and 100 µl of the Antibody Solution (Prepared by mixing 5 µl of antibody with 95 µl of wash buffer) per section was placed and incubated for 30 min at room temperature. Nuclear staining was achieved by adding 100 µl of Propidium Iodide/Rnase A solution for 30 min followed by

washing in distilled water. Anti-Fade solution (Vectamount, Vector Labs, USA) was added as mountant. The slides were visualized by Laser Scanning Confocal Microscope (LSM 510META, ZEISS, Germany) using Argon and Krypton Lasers. Optical slices were taken at ~ 0.8μm. Laser gains, pin hole setting and magnification were set identical across samples. Apoptotic cells exhibited strong nuclear green fluorescence (Alexa fluor 488: λ_{ex}: 499, λ_{emi}: 519) while PI staining exhibited strong red counter stain (Propidium Iodide: λ_{ex}: 536, λ_{emi}: 617).

Results:

Qualitative and quantitative analysis of OI extracts:

Preliminary qualitative phytochemical analysis of aqueous extract of OI showed the presence of phenols, saponins, tannins, terpenoids, sterols and carbohydrates while, alkaloids, anthroquinones and amino acids tested negative.

Phytochemical analysis : Preliminary phytochemical analysis showed the presence of phenols, flavonoids, saponins, tannins, terpenoids, sterols, carbohydrates, while alkaloids, anthraquninones and amino acids were found to be absent. Quantitative analysis revealed the presence of phenols (64.81±1.51 mg/g), flavonoids, (72.8±1.87 mg/g), tannins (22.76±0.72 mg/g), and saponins (106.4±2.81 mg/g).

Qualitative phytochemical analysis was performed using TLC to identify alkaloids, terpenoids, flavonoids and steroids. Methanolic extract was chosen as, most compounds are separated in this fraction. For non-polar compounds, petroleum ether extract was selected. Methanolic extract showed at least 15 spots in visible light, UV_{254} and UV_{366} (fig.1A,B,C). The TLC chromatogram of the leaf extract was dominated by chlorophyll and its degradation product (Red fluorescence under UV_{365} nm). Derivitization with anisaldehyde, Dragendorf and NBT reagent revealed the presence of terpenoids, (fig.1D), alkaloids (fig.1E) and steroids (fig.1F). The flavonoidal fraction was subjected to Co-TLC with known flavonoids which revealed the presence of atleast 4 flavonoids (fig. G,H, I, J)

GC-MS (Fig 2a): Hexane extract revealed the presence of (1) Hentriacontane, RT: 34.34 (m/z : 436, $C_{31}H_{64}$, 53.76%), (2) Beta sitosterol acetate RT: 41.60 (m/z 456,

$C_{31}H_52O_2$, 2.68%), (3) Azulene, RT: 43.93 (m/z: 204,$C_{15}H_{24}$, 2.03%), (4) Phytol, RT: 21.84 (m/z: 296, $C_{20}H_{40}O$, 1.72%), (5) Triacontane RT: 37.32 (m/z: 422, $C_{30}H_{62}$,2.20%), (6) Docosane, RT: 41.14 (m/z: 310,$C_{22}H_{46}$, 14.37%), (7) Squalene, RT: 28.69(m/z: 410, $C_{30}H_{50}$, 3.97%), (8) Hexatriacontane. RT: 28.99 (m/z: 506, $C_{36}H_{74}$, 15.92) and (9) Tritetracontane: RT: 31.90 (m/z: 604, C43H88, 1.39%) (Figure: 2 A, B, C, D).

Non-Polar Compounds (Fig. 2b): Fraction 3 afforded a oil like compound (**1**) (0.23ml) while, fraction 12 on crystallization with acetone yielded compound (**2**) beta sitosterol (210.3 mg) and fraction 16,18 yielded two compounds (**3, 4**) identified as hentriacontane and tricontanol acetate, based on spectroscopic analysis (Figure 2E).

Compound **4** was obtained as a white solid on crystallization with methanol, with a mp 82-85 °C. Its ^{1}H NMR spectrum indicated it to be aliphatic in nature. The absence of a molecular ion peak in the mass spectrum and the presence of a peak at *m/z* 420 for (M^+ - H_2O) indicated that it contained a hydroxyl group and was therefore analyzed for $C_{30}H_{62}O$. The presence of a hydroxyl group was further supported by its ^{13}C NMR spectrum, which showed a signal at δ 63.04 for the carbon carrying the hydroxyl group. The presence of a hydroxyl group was further confirmed by its IR spectrum, which showed a broad absorption band at 3398 cm^{-1}. Its ^{1}H NMR spectrum exhibited signals for the presence of a terminal methyl group at δ 0.88 and a chain of methylene protons at δ 1.26. A triplet at δ 3.63 showed the presence of a methylene linked to the oxygen. All of these spectral data, when coupled together, indicated compound **4** to be a saturated primary alcohol containing C_{30} carbon atoms. On the basis of the above spectral studies, compound **4** was characterized as triacontanol. The

proposed structure was confirmed by analyzing its acetate **4(a)**, prepared by acetylating **4** with AC_2O/pyridine under dry conditions.

The IR spectrum of **4(a)** showed absorption at 1731 cm^{-1} confirming the formation of an ester. Its ^1H NMR showed a singlet at δ 2.04 integrating for three protons and a triplet at δ 4.05 integrating for two protons, corresponding to the acetyl group and α-hydroxymethylene, respectively. Thus, on the basis of the spectral data of **4** and its acetate **4(a)**, compound **4** was identified as triacontanol.

Triacontanol (4). White solid, mp 82-85 °C. IR V_{max} (KBr): 3398, 2918, 2849, 1463, 1360, 1061, 720 cm^{-1}. ^1H NMR (δ , $CDCl_3$, 300 MHz): 0.88 (t, 3H, $-CH_3$), 1.26 (brs, 54H), 1.54 (m, 2H, $-CH_2CH_2OH$), 3.63 (t, 2H, $-CH_2OH$). ^{13}C NMR (δ, $CDCl_3$, 75.47 MHz): 14.01 ($-CH_3$), 25.67-32.76 ($-CH_2$), 63.04 ($-CH_2OH$). EIMS *m/z* (%): 420 (M^+ - 18, 36), 392 (8), 364 (5), 167 (18), 153 (20), 125 (950), 57 (100).

Triacontanol Acetate 4(a). White solid, mp 68-70 °C. IR V_{max} (KBr): 2917, 2849, 1731, 1473, 1463, 1367, 1239, 1043, 756, 729, 719 cm^{-1}. ^1H NMR (δ, $CDCl_3$, 300 MHz): 0.88 (t, 3H, $-CH_3$), 1.27 (brs, 54H), 1.61 (m, 2H, H-2), 2.04 (s, 3H, $-COCH_3$), 4.05 (t, 2H, $-CH_2O$).

HPLC: For qualitative fingerprint analysis of flavonoidal rich fraction (FRF) (Fig. 3: A, B), commonly known flavonoids/glycosides (from family Urticaceae and genus: *Oreocnide*) were chosen as marker flavonoids based on literature, since there are no chemical constituents reported from *Oreocnide integrifolia*. High performance thin layer chromatographic analysis revealed the presence of at least four flavonoids when derivatized with NP-PEG reagent. Co-TLC with standards depicted the presence of

rutin and/or quercetin. Hence, we planned to identify these flavonoid markers using high pressure liquid chromatography (HPLC) and compare the retention times (RT) with that of FRF. The chromatogram of flavonoid rich fraction was run over 30 min until no sharp peaks were detected (Figure: 3A, B). The retention time of standard markers, morin (Fig. 3: C), rutin (Fig. 3: D), apigenin (Fig. 3: E) and quercetin (Fig. 3: F), in chromatographic condition I were found to be at 9.170, 5.473, 23.147 and 5.480 min, respectively (Figure: 3C, D, E, F).The FRF chromatogram showed peak at 5.457 min corresponding to the retention time of rutin and quercetin (Figure: 3G).

Further, another chromatographic condition was optimized to get separation of compounds which were not detected or did not separate under chromatographic I set up. This chromagram of FRF showed 11 prominent peaks in 25 min run time (Figure 3H,I). The retention time of kaempherol (Fig. 3: J, K), hesperidin (Fig. 3: L), naringin (Fig. 3: M), quercetin (Fig. 3: N), and rutin (Fig. 3: O), were found to be 9.573, 5.383, 4.967, 3.663 and 3.663 min, respectively. The chromatogram of FRF showed a peak at 9.563 min corresponding to the retention time of kaempherol (Figure 3: K). Also, FRF chromatogram showed peaks at 5.300, 5.000 and 3.700 min corresponding to the retention time of hesperidin, naringin and quercetin/rutin (Figure 3 P, Q). A total of around 13 compounds were detected in the FRF and hence, from the chromatograms recorded under chromatographic set up II, it can be concluded that, our FRF may contain kaempherol, hesperidin, naringin and rutin or quercetin. However, a detailed scrutiny would be required by using LC-MS/MS signatures, which could help in the enumeration of the complete flavonoid profile.

Glucose stimulated insulin secretion (GSIS) for isolated islets by aqueous OI extract (Table 1):

Insulin secretion under basal glucose concentration of 4.5 mM showed no effect of the lowest dose of 10μg/ml of OI extract while, 50, 100 and 250μg/ml doses exerted significantly augmented insulin release with the latter two doses being equally effective for maximal secretion (35%).

In contrast to basal secretion, stimulated secretion under a glucose concentration of 16.7 mM showed significant dose dependent increment by 16% with 10μg/ml, 29% with 50μg/ml, 44% with 100μg/ml and 63% with 250μg/ml of OI extract.

GSIS of various solvent extracts from RIN m 5F cell line (Fig. 4):

Except for the ethyl acetate and methanol fractions, which showed a dose dependent increase in insulin release, none of the other fractions showed any noticeable effect on insulin release under basal (4.5mM glucose) glucose concentration.

Under higher concentration of ambient glucose, both ethyl acetate (2-3 fold) and methanol (3-4 fold) fractions showed significant dose dependent increment in insulin release. In addition, both chloroform and butanol fractions also depicted some degree (1.5 fold) of increment in insulin release, especially with the higher dose.

Promotion of 2NBDG glucose uptake by various solvent extracts in C2C12 cells (Fig. 5):

Basal glucose uptake was significantly less in presence of all solvent fractions compared to insulin. However, ethyl acetate and methanol fractions show dose dependent increment in glucose uptake which are significantly greater than other fractions tested. However, higher concentration of butanol fraction showed maximal glucose uptake compared to both ethyl acetate and methanol fractions.

Even though all fractions showed dose dependent increment in glucose uptake in presence of insulin, it was still lesser compared to insulin alone, except for the higher dose of ethyl acetate fraction and both doses of methanol fraction, which showed maximal glucose uptake more than that shown by insulin.

GSIS from RIN m 5F cells by FRF fraction (Fig. 6):

Under both basal (4.5mM) and higher (16.7mM) glucose ambient concentration, the FRF fraction depicted a dose dependent increment in insulin secretion with the highest dose showing almost doubled insulin secretion.

FRF stimulated 2NBDG glucose uptake by C2C12 cells (Fig. 7):

The FRF fraction depicted a dose dependent 5-15 fold increase in glucose uptake even in the absence of insulin. The insulin induced glucose uptake was further stimulated 2-5 fold in a dose dependent manner by the FRF fraction.

GSIS by FRF from isolated mouse islets (Fig. 8):

The FRF, induced significant dose dependent increment in insulin secretion from mouse islets under both basal (4.5mM) and stimulated (16.7mM) glucose concentrations. The increment in insulin release under glucose challenge was significantly greater than in the basal state. The highest dose of FRF showed near 45% increase in GSIS.

Effect of FRF on glucose induced increase in cAMP and Ca^{++} levels in islets (Fig. 9, 10):

There was no increase in intra islet cAMP or Ca^{++} on exposure to any of the doses of FRF under basal ambient glucose level. However, under stimulating concentration of glucose, a dose dependent increment by FRF in intra islet cAMP and Ca^{++} levels could be noticed. Further, this dose dependent effect of FRF on cAMP and Ca^{++} levels could be discerned in a medium containing less stimulating concentration (11.1 mM) of glucose and the PDE inhibitor IBMX.

***In-vitro* assessment of the effect of FRF on streptozotocin induced islet viability and oxidative stress:**

All oxidative stress parameters, MTT (Fig. 11), DCF (Fig. 12), Peroxynitrite (Fig. 13), NO (Fig. 14), Rh 123 (Fig. 15), and LPO (Fig. 16), were all significantly elevated in presence of streptozotocin. FRF protected the islets against STZ induced oxidative stress in a dose dependent manner with the highest dose affording near total

protection. Streptozotocin significantly reduced cell viability which was protected against by the co-presence of FRF in a dose dependent mode.

Assessment of the anti-diabetic potential of FRF in multidose STZ mice:

Blood glucose and insulin level (Fig. 17, 18):

Streptozotocin diabetic mice showed significant hyperglycemia and hypoinsulinemia. FRF treated mice showed significant increase in plasma insulin and concomitant decrease in glucose in a dose dependent manner.

Histological observations (Plate 1-3):

The pancreatic islets of streptozotocin administered mice depicted β-cell loss and larger spaces within due to β-cell toxicity of STZ. FRF supplementation showed recovery of the structural integrity of islets with the pancreas of mice administered highest dose of FRF depicting near normal islet histoarchitecture.

Immunocytochemistry of pancreatic islets for cellular apoptosis and insulin (Plate 4, Fig 19):

The pancreatic islets of STZ treated mice depicted greater number of TUNEL positive cells and on quantitative terms a six fold higher percentage of apoptotic cells. Pancreatic islets of STZ treated mice demonstrated reduced immunoreactivity for insulin while, the islets of FRF supplemented mice showed increased insulin immunoreactivity, with 250 μg FRF treated islets showing strong immunoreactivity.

Fig 1:HPTLC fingerprint of Methanolic extract of *Oreocnide integrifolia*

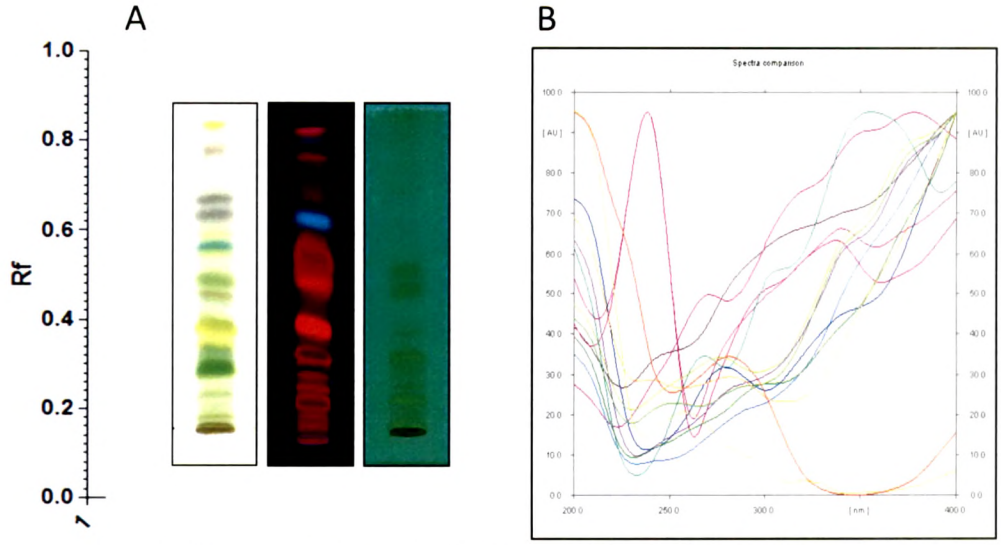

C: Densitometric scan at visible light of Methanolic extract

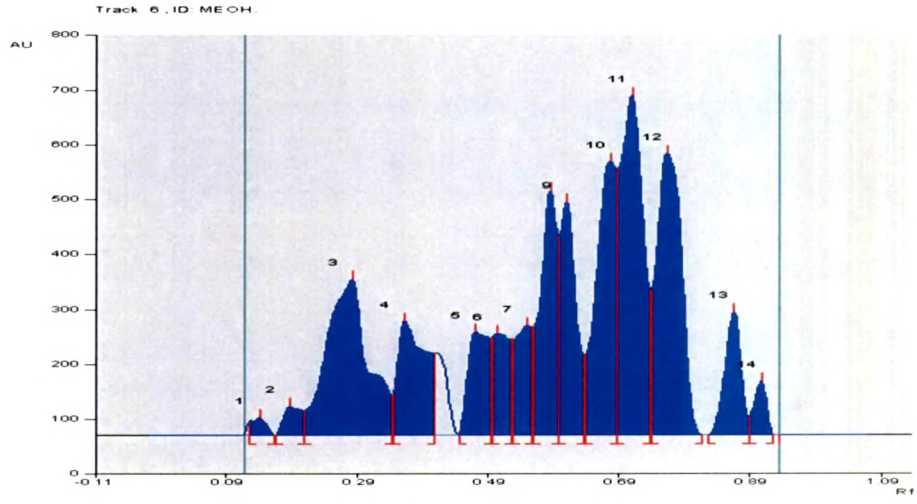

Solvent system : Chloroform : Methanol (95:05)

Fig. 1:Derivitization of various fractions for alkaloids, terpenoids, steroids

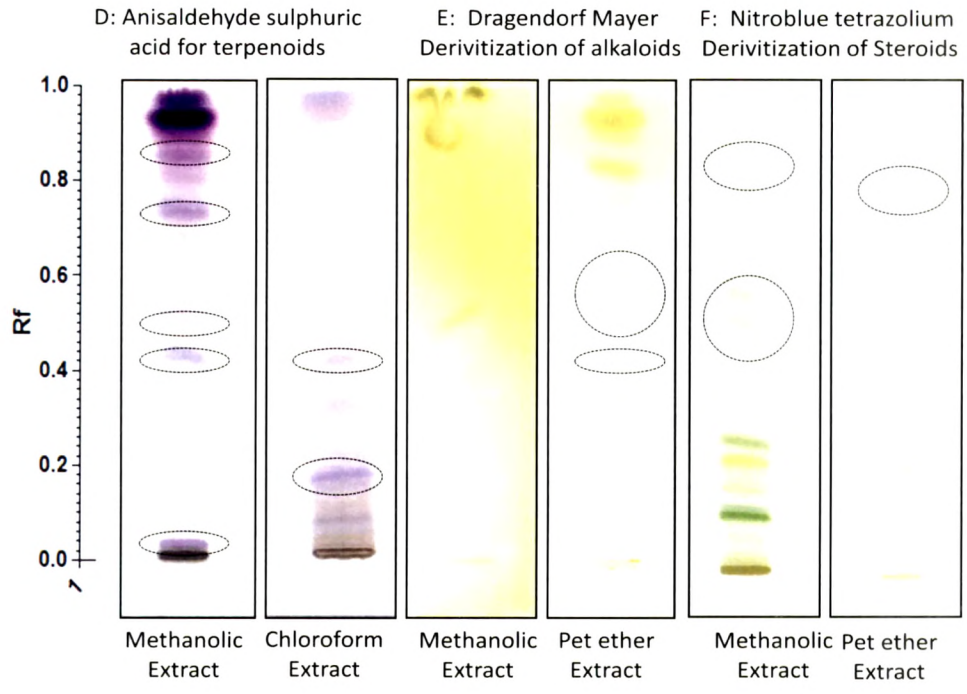

Mobile Phase : Chloroform : Methanol (95:05)

Fig. 1:G: HPTLC detection of flavonoids derivitized with NP-PEG reagent (Visible)

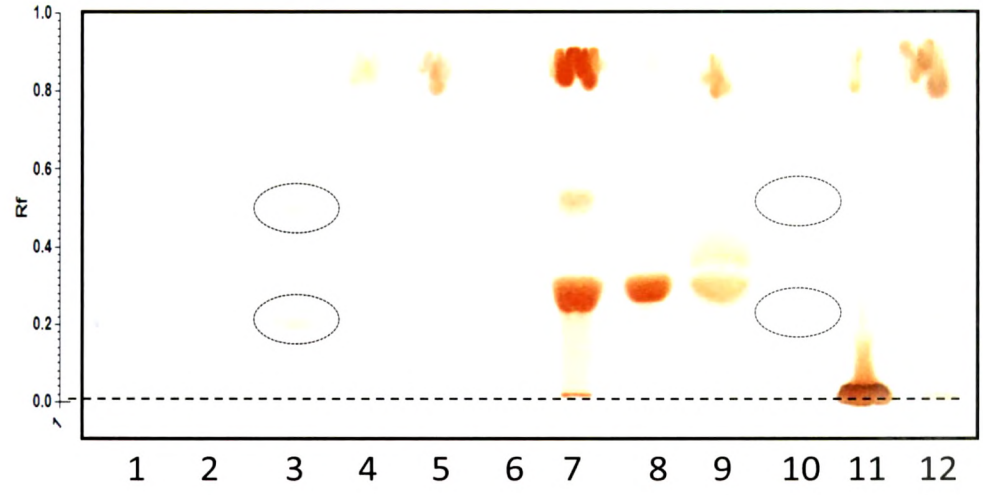

H: HPTLC detection of flavonoids derivitized with NP-PEG reagent UV-254nm

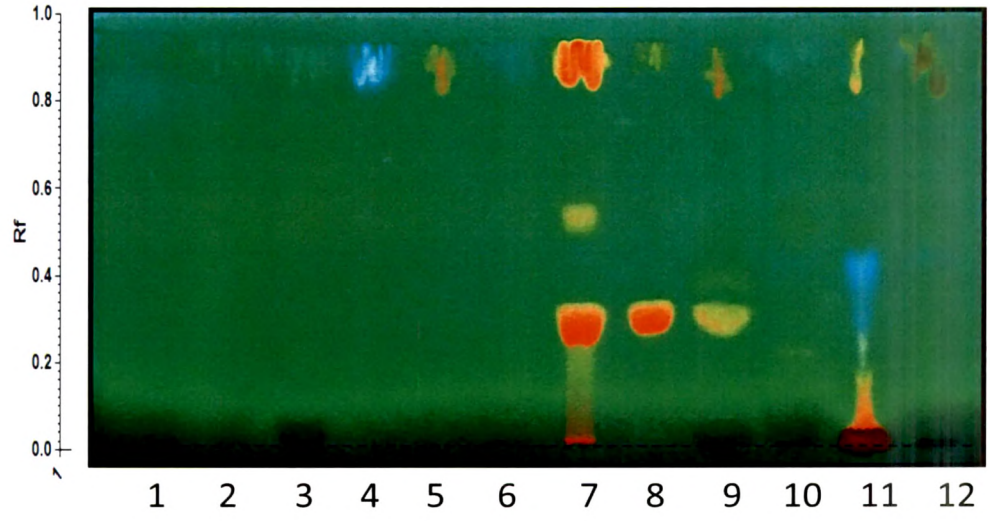

1 = Apigenin, 2= Naringin, 3 = FRF, 4 = Morin , 5 =Kaempherol, 6 = Chrysin , 7= Quercetin, 8 = Rutin, 9 = Hesperidin, 10 = FRF, 11= BuOH, 12 = $CHCl_3$

Solvent system: Ethyl acetate: formic acid: glacial acetic acid : water
100 : 11 : 11 : 26

Fig. 1: I: HPTLC detection of flavonoids derivitized with NP-PEG reagent UV-366nm

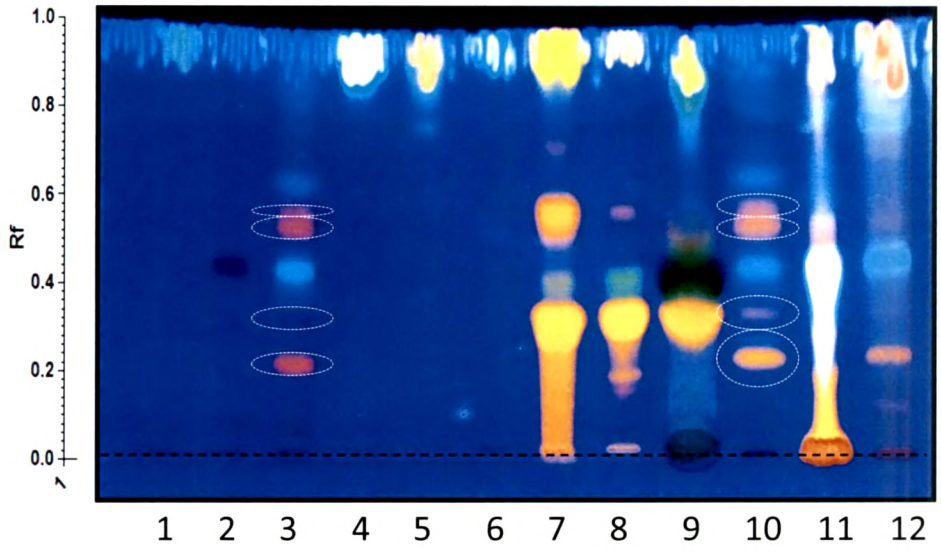

1 = Apigenin, 2= Naringin, 3 = FRF, 4 = Morin , 5 =Kaempherol, 6 = Chrysin , 7= Quercetin, 8 = Rutin, 9 = Hesperidin, 10 = FRF, 11= BuOH, 12 = $CHCl_3$

C: Densitometric scan at UV-366 of flavonoid rich fraction

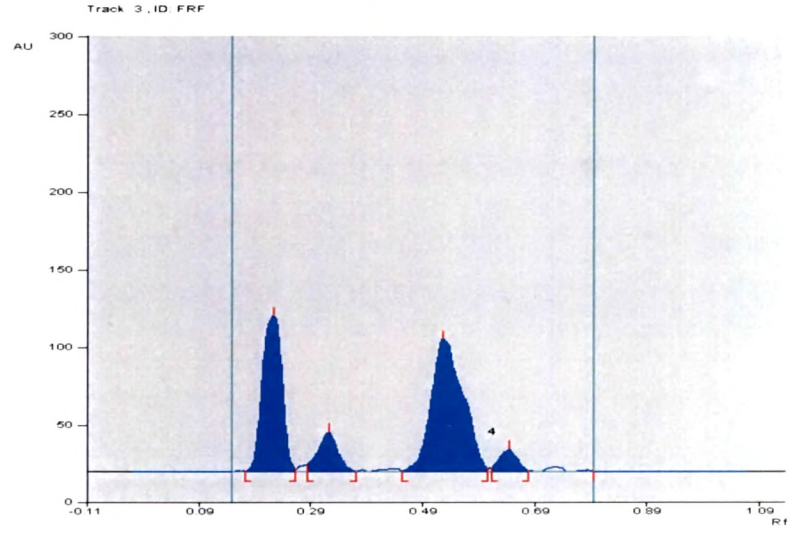

Solvent system: Ethyl acetate: formic acid: glacial acetic acid : water

100 : 11 : 11 : 26

Fig. 2a: Gas Chromatography linked Mass Spectroscopy

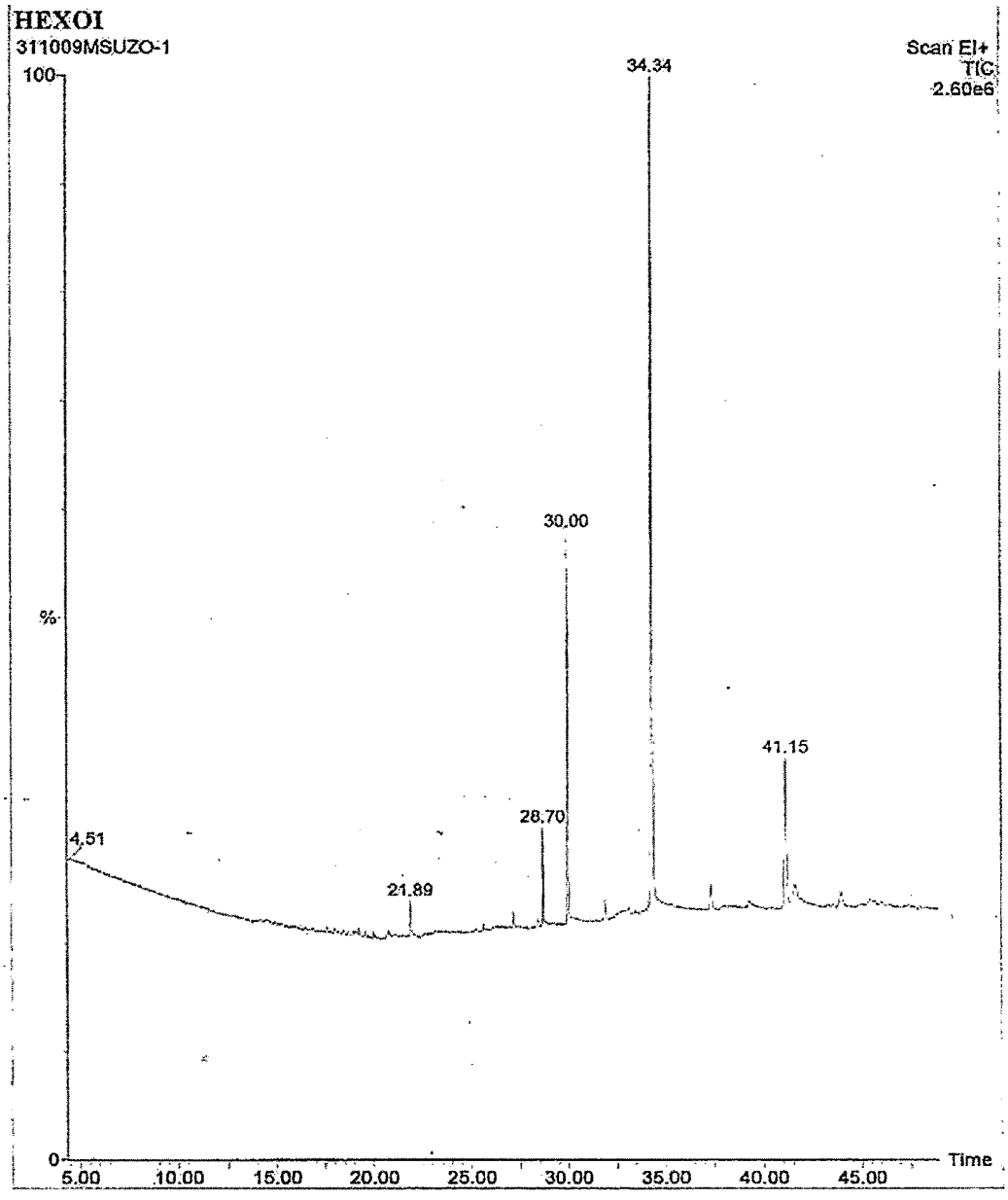

Total Ion Chromatogram of Hexane fraction of *Oreocnide integrifolia*

Fig 2b: Non-polar chemical constituents from hexane fraction

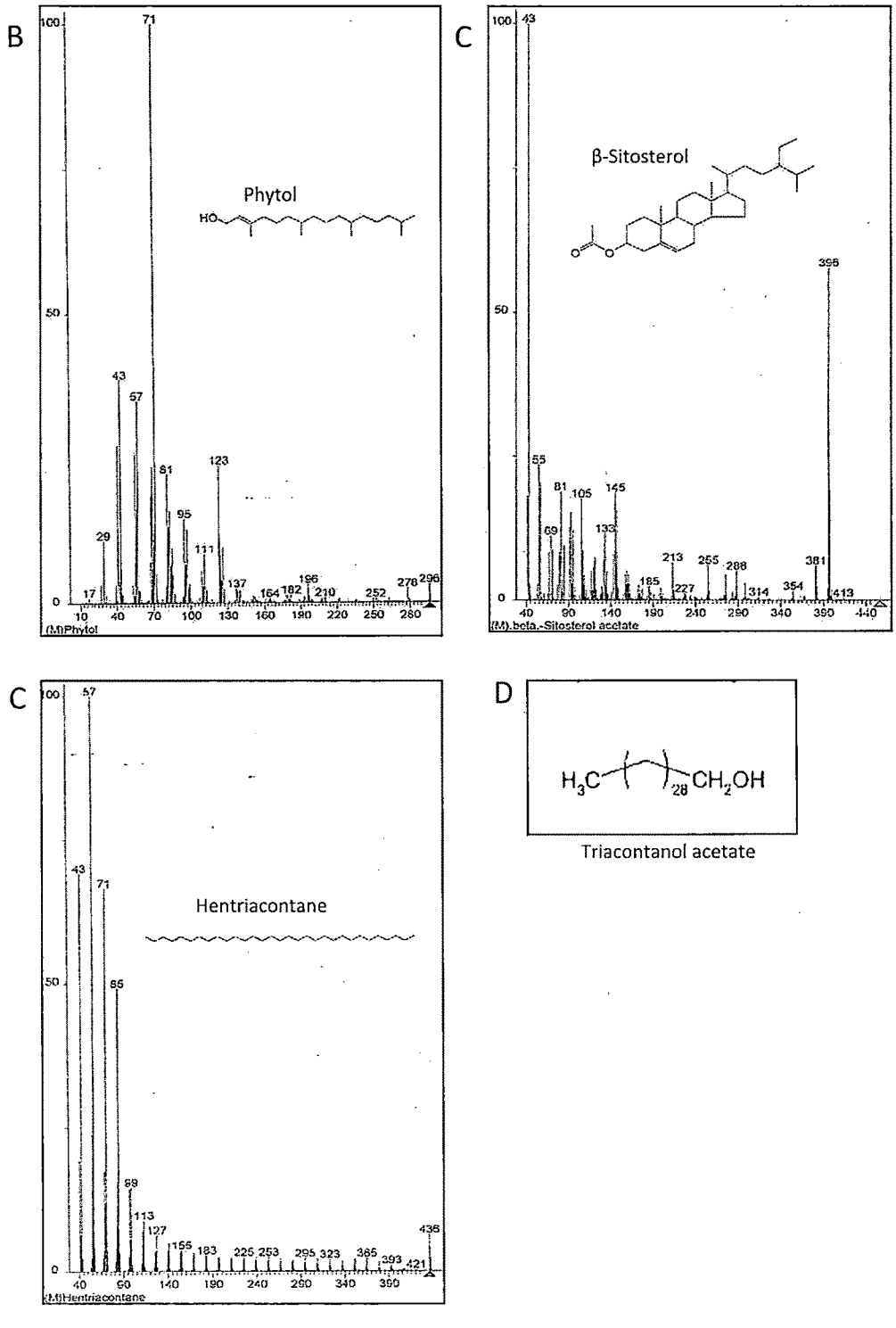

Fig 3 : HPLC chromatograms of Flavonoid rich fraction and flavonoid marker : Chromatographic condition I

A: HPLC chromatogram of Flavanoid rich fraction

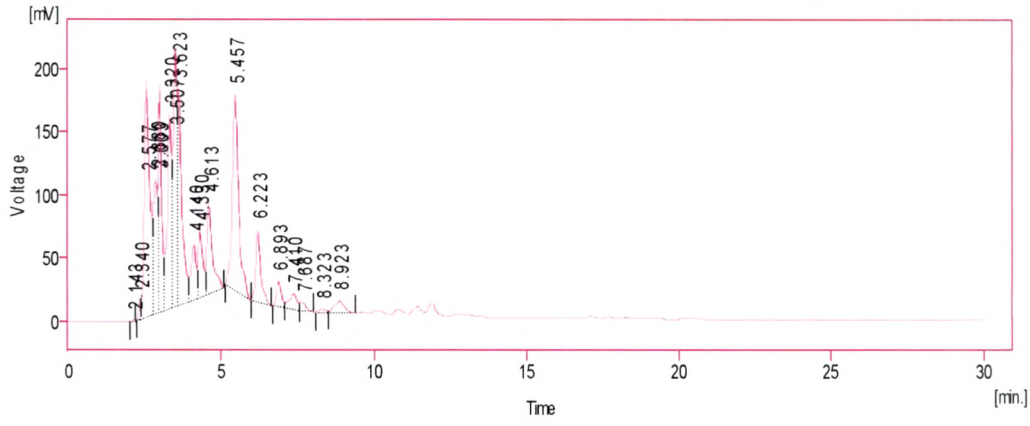

B: HPLC chromatogram of Flavanoid rich fraction: magnified

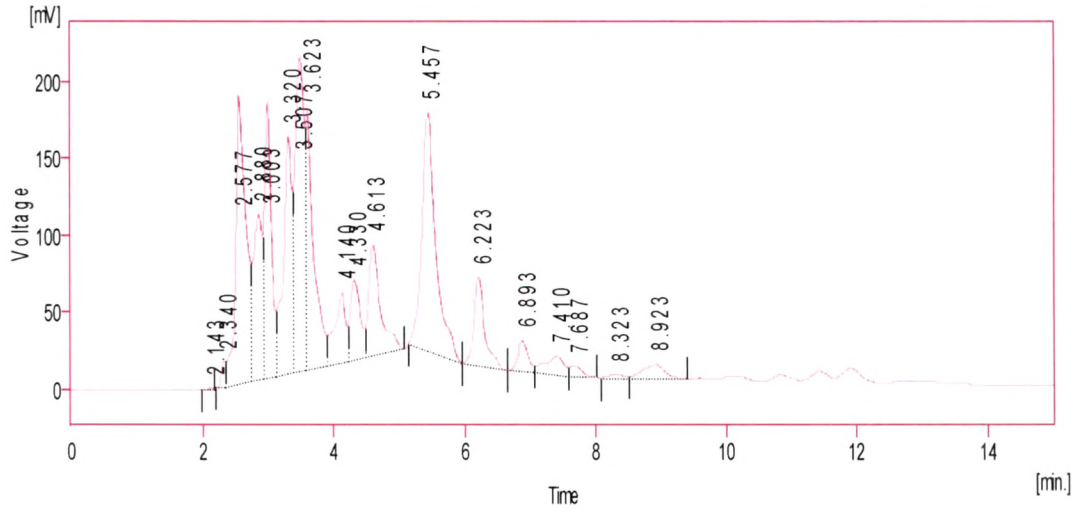

Fig. 3 : HPLC chromatograms of Flavonoid rich fraction and flavonoid marker : Chromatographic condition I

C: HPLC chromatogram of Morin

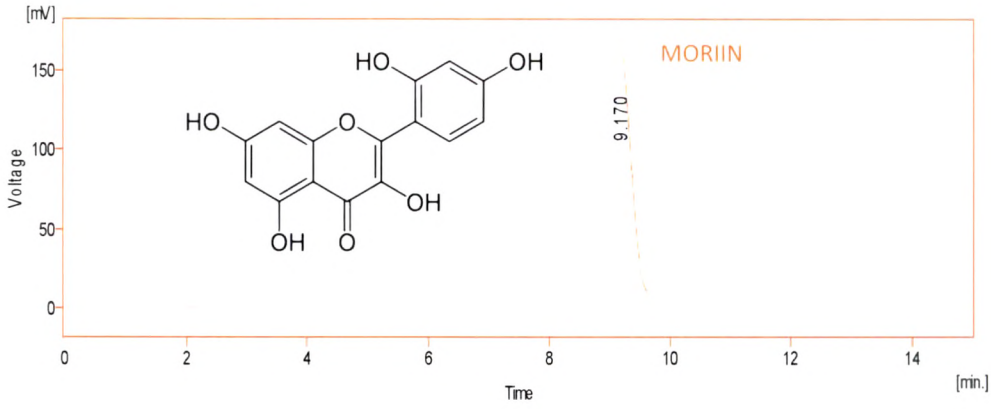

D HPLC chromatogram of Rutin

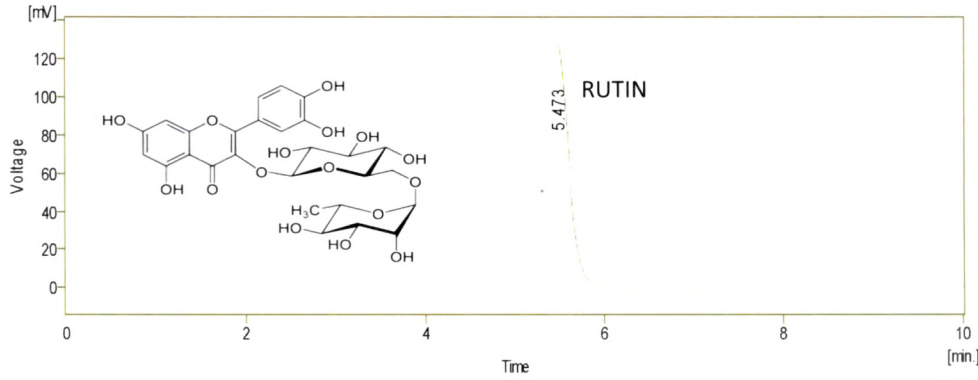

E: HPLC chromatogram of Apigenin

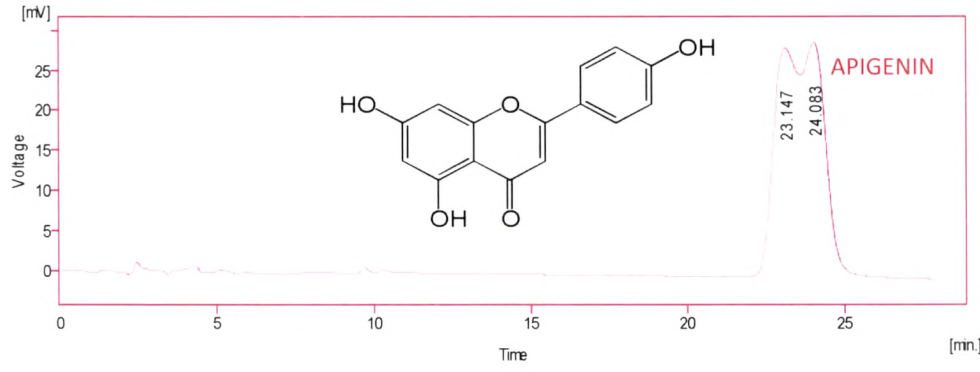

Fig. 3 : HPLC chromatograms of Flavonoid rich fraction and flavonoid marker : Chromatographic condition I

F : HPLC chromatogram of Quercetin

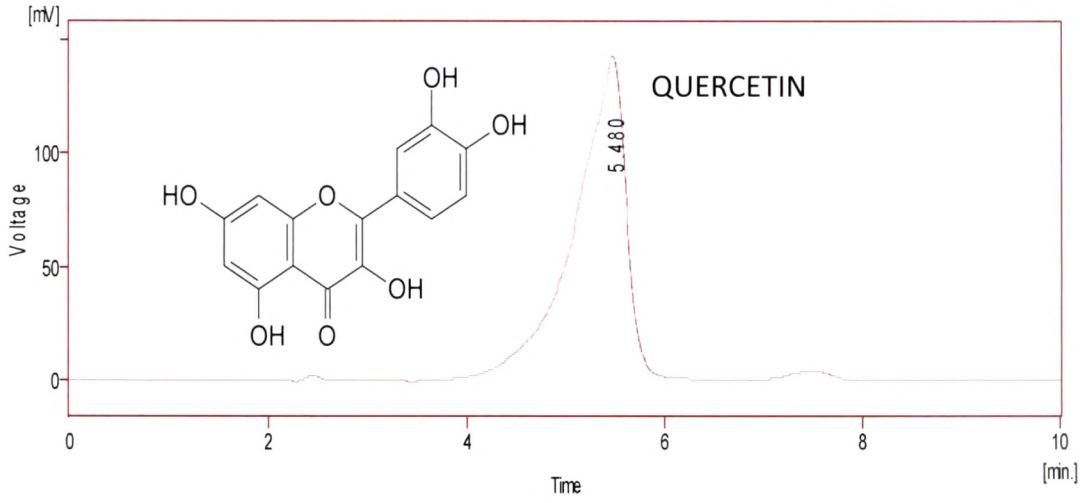

G : HPLC chromatogram of Rutin and FRF overlay

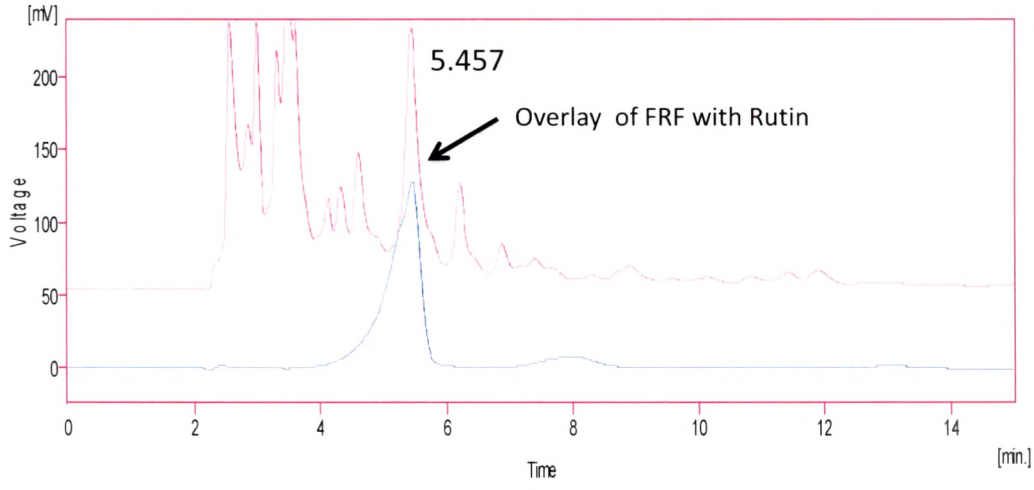

Fig. 3: HPLC chromatogram of Flavanoid rich fraction and flavonoid markers In chromatographic condition II

H: HPLC chromatogram of Flavanoid rich fraction

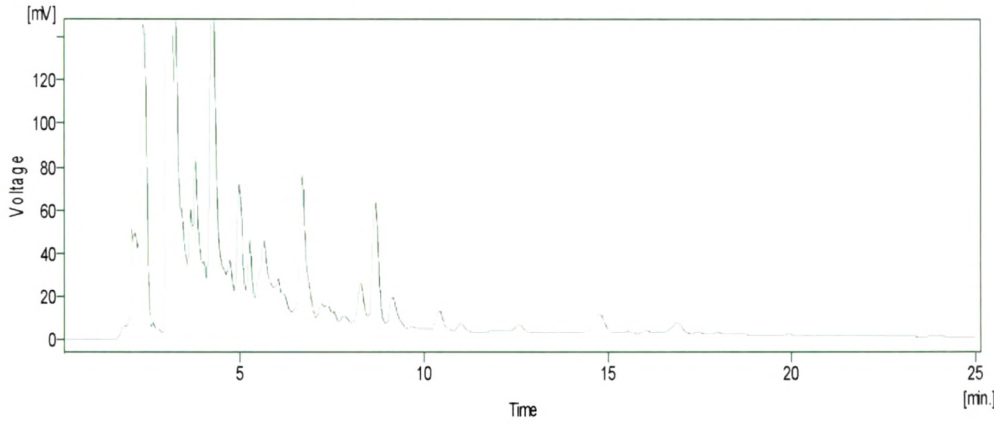

I: HPLC chromatogram of Flavanoid rich fraction (magnified)

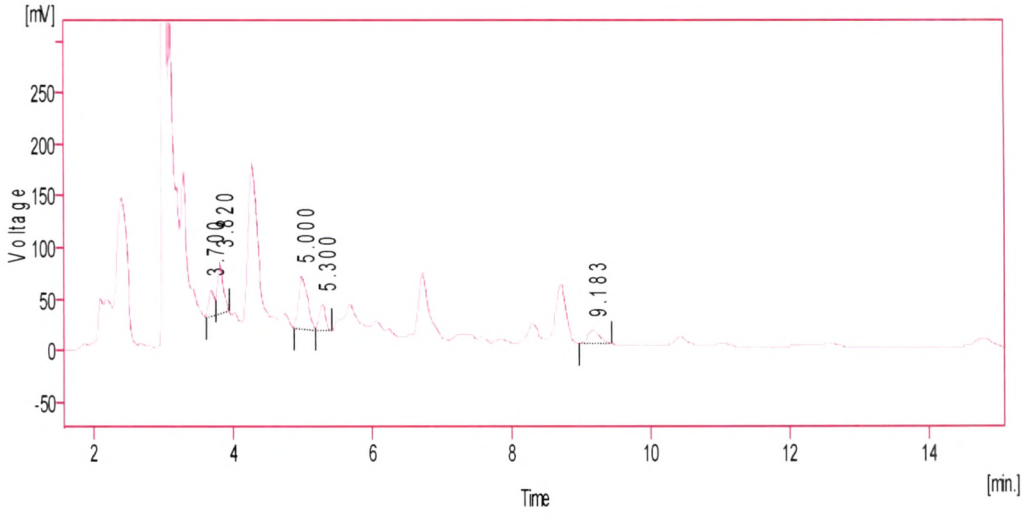

Fig. 3: HPLC chromatogram of Flavanoid rich fraction and flavonoid markers In chromatographic condition II

J : HPLC chromatogram of Kaempherol

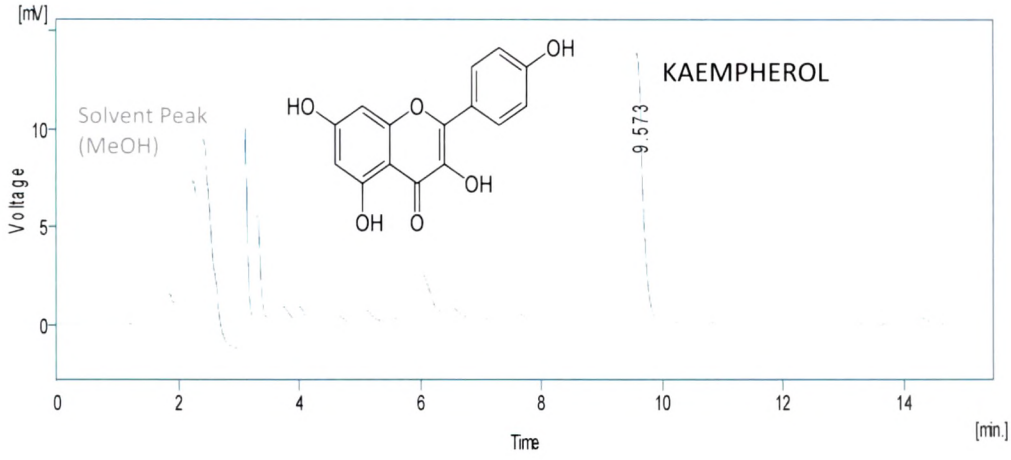

K: HPLC chromatogram of Kaempherol

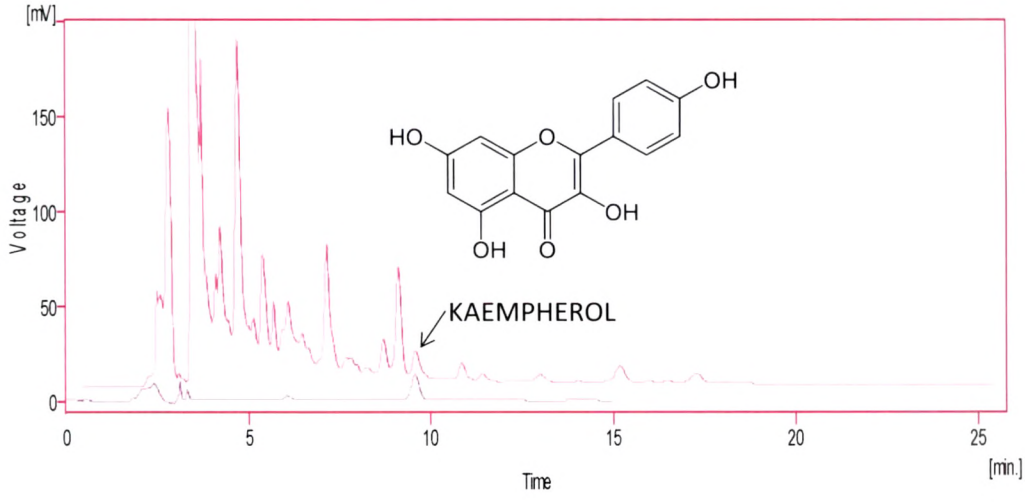

Fig. 3: HPLC chromatogram of Flavanoid rich fraction and flavonoid markers In chromatographic condition II

L : HPLC chromatogram of Hesperidin

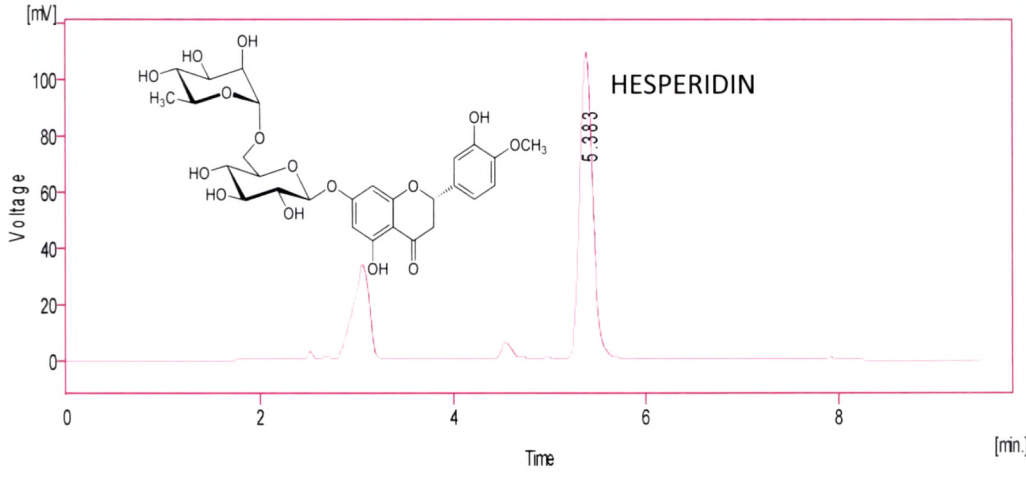

M: HPLC chromatogram of Naringin

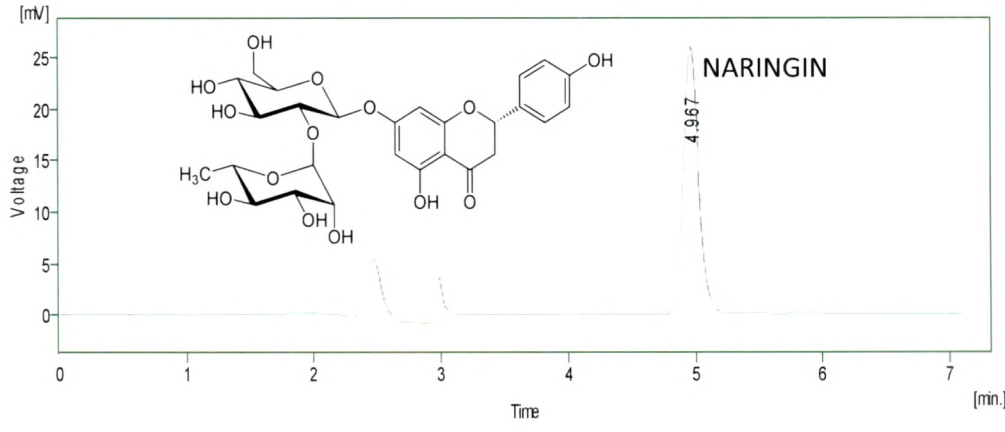

Fig. 3: HPLC chromatogram of Flavanoid rich fraction and flavonoid markers In chromatographic condition II

N: HPLC chromatogram of Quercetin

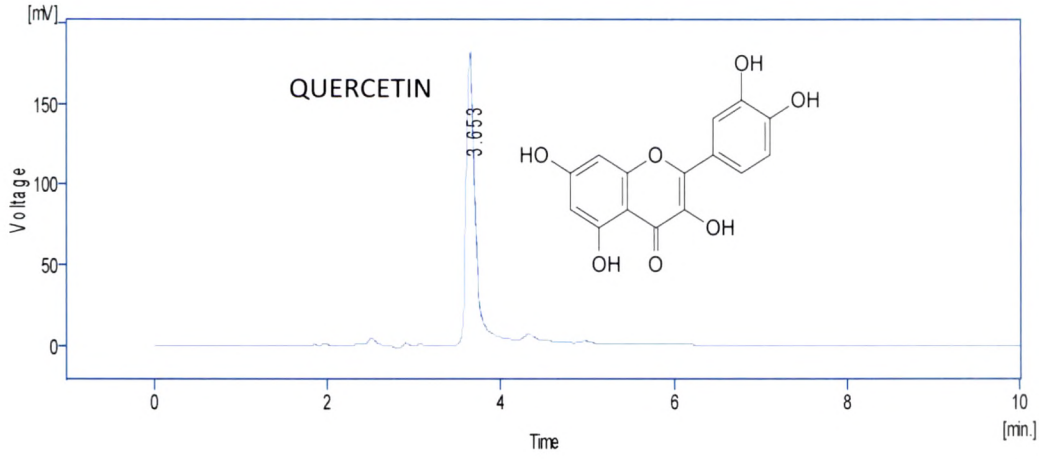

O : HPLC chromatogram of Rutin

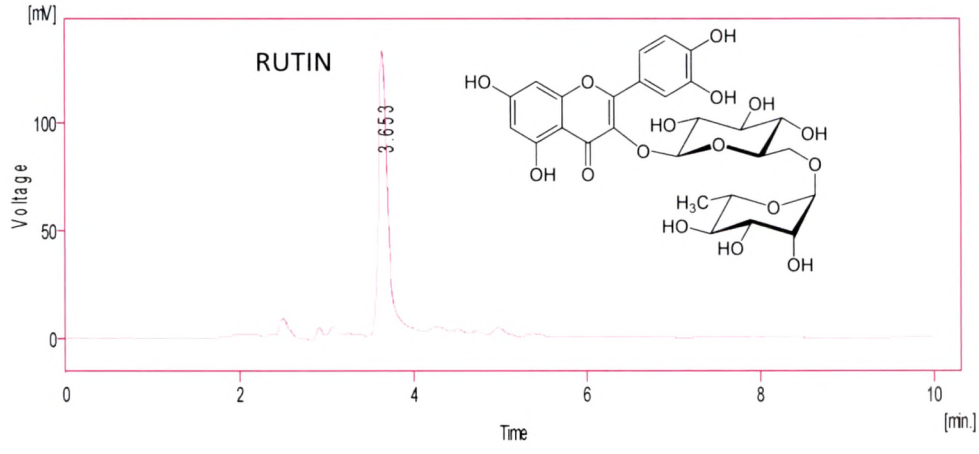

Fig. 3: HPLC chromatogram of Flavanoid rich fraction and flavonoid markers In chromatographic condition II

P : HPLC chromatogram of Standard mixture

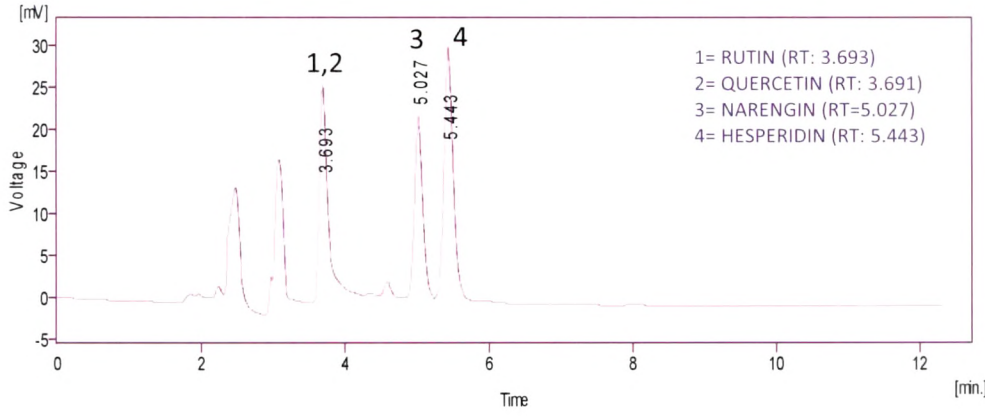

Q: HPLC chromatogram of standard and FRF overlay

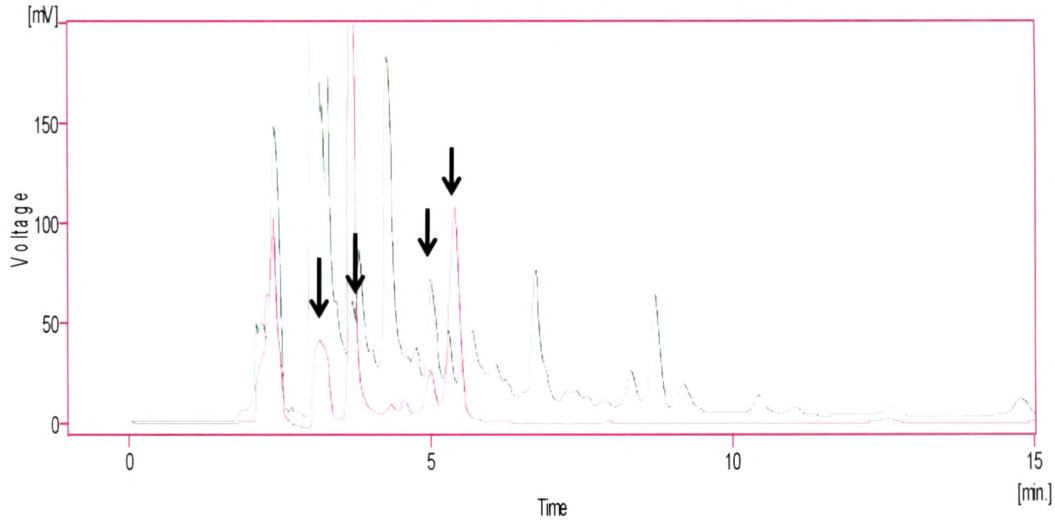

Table 1: GSIS of water OI extract in mouse islets

	4.5mM Glucose	**16.7mM Glucose**
	pmol/L per 100 islets	pmol/L per 100 islets
Control	50.0 ± 1.66	87.5 ± 3.31
10ug/ml OI extract	47.7 ± 1.94	101.3 ± 1.31**
50ug/ml OI extract	61.3 ± 2.15*	112.4 ± 1.80**
100ug/ml OI extract	68.4 ± 1.52**	125.6 ± 1.30**
250ug/ml OI extract	67.0 ± 2.10*	142.9 ± 0.83**

All values were expressed as mean ± SEM of 5 independent experiments .Significance levels were expressed as * P< 0.01 when compared to respective controls and ** P< 0.01 when compared to respective controls

Fig. 4:Effect of different fractions in GSIS in RINm5F cell line

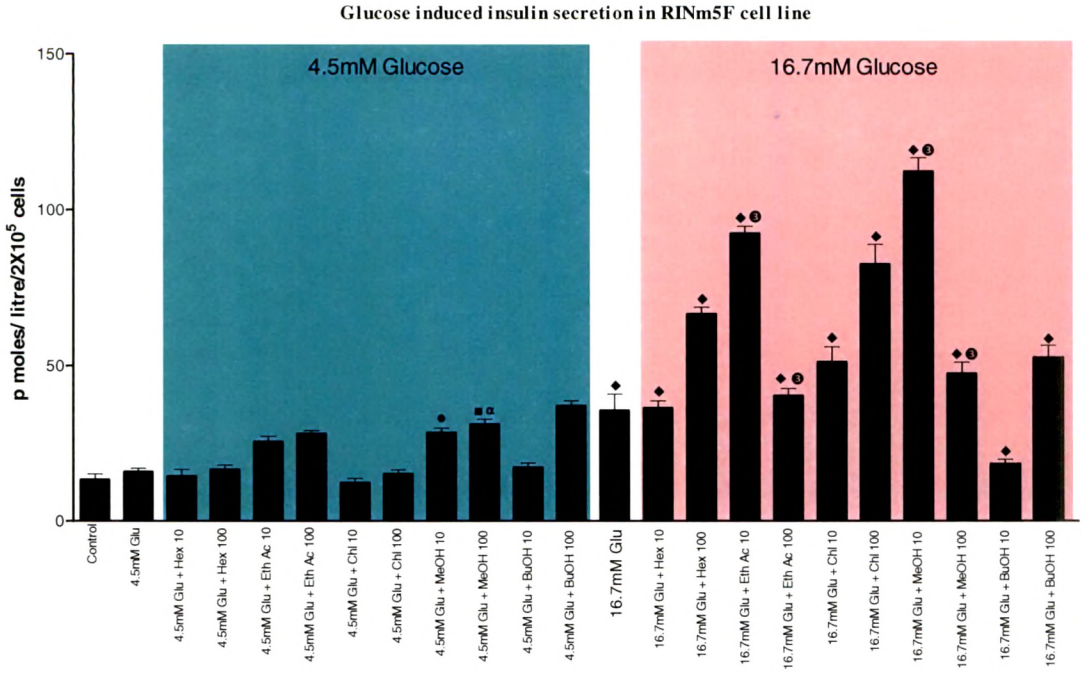

●=p<0.01, ■=p<0.001, ◆=p<0.0001: Control was compared with rest of the groups
α = p <0.05, β = p <0.01, δ = p <0.001: 4.5mM glucose was compared to rest of the groups
❶ = p <0.05, ❷ = p <0.01, ❸= p <0.001: 16.7mM glucose was compared to rest of the groups

Fig. 5 :Effect of different fractions on glucose upkate in C2C12 cell line

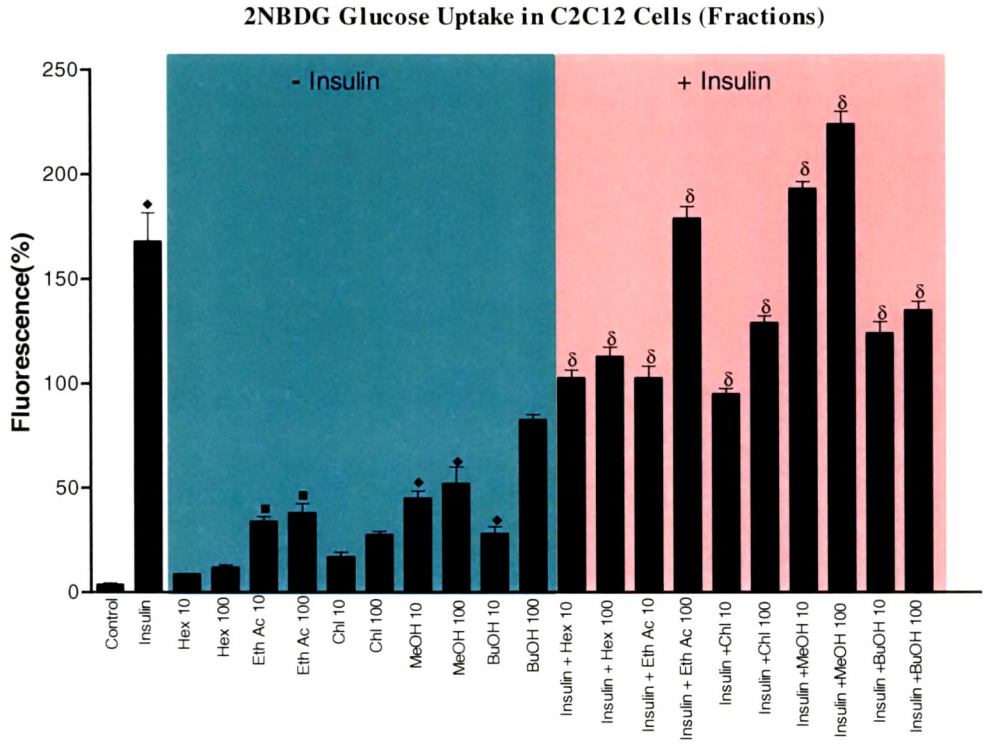

●=p<0.01, ■=p<0.001, ◆=p<0.0001: Control was compared with rest of the groups
α=p<0.01, β=p<0.001, δ=p<0.0001: Insulin was compared with rest of the groups

Fig. 6:Effect of flavonoidal fraction in GSIS in RINm5F cell line

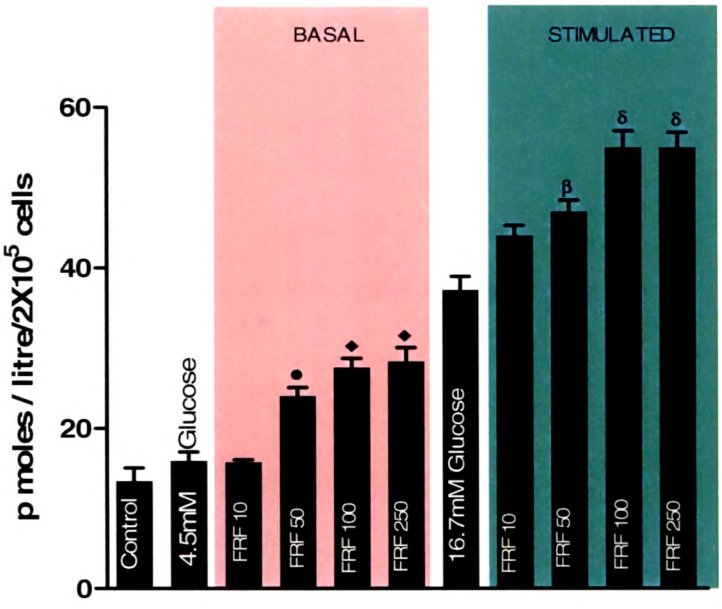

● = p < 0.05, ■=p <0.01, ◆=p < 0.001:4.5mM glucose was compared to FRF 10,50,100,250

α = p <0.05, β = p <0.01, δ = p <0.001:16.7mM glucose was compared to FRF 10,50,100,250

Fig. 7 Effect of FRF on glucose uptake in C2C12 cell line

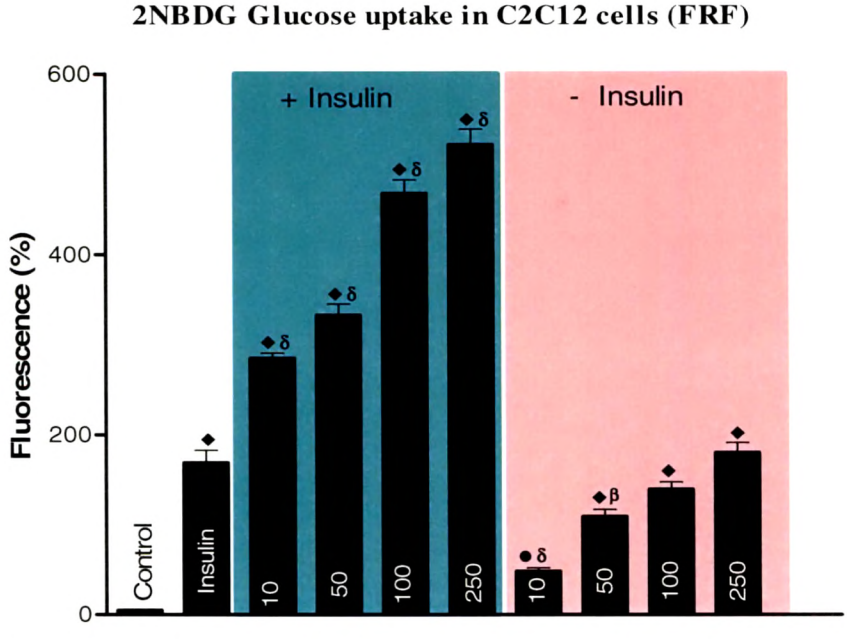

●=p<0.01, ■=p<0.001, ◆=p<0.0001: Control was compared with rest of the groups

α=p<0.01, β=p<0.001, δ=p<0.0001: Insulin was compared with rest of the groups

Fig. 8: Effect of FRF is isolated mouse islets

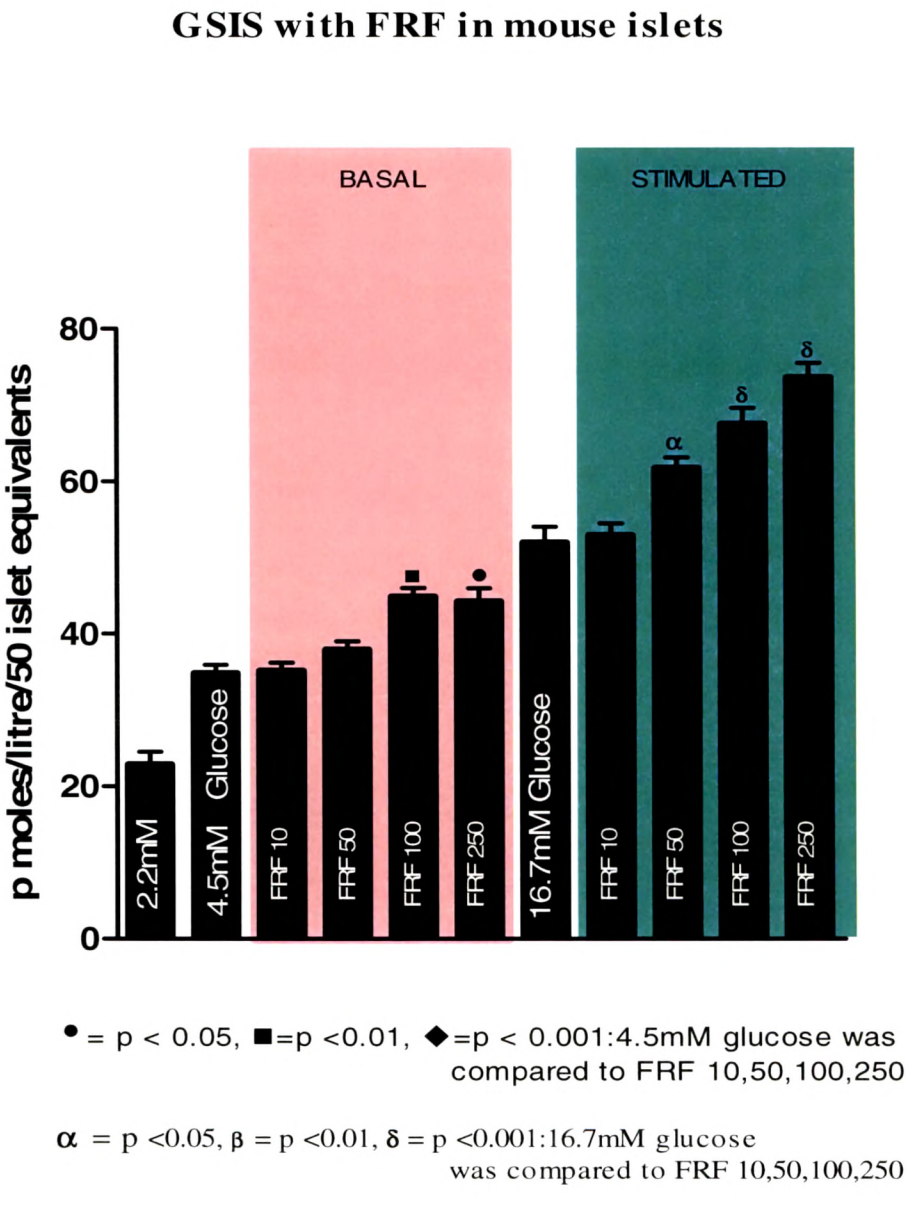

● = p < 0.05, ■=p <0.01, ◆=p < 0.001:4.5mM glucose was compared to FRF 10,50,100,250

α = p <0.05, β = p <0.01, δ = p <0.001:16.7mM glucose was compared to FRF 10,50,100,250

Fig. 9: Effect of FRF on cAMP levels in mouse islets

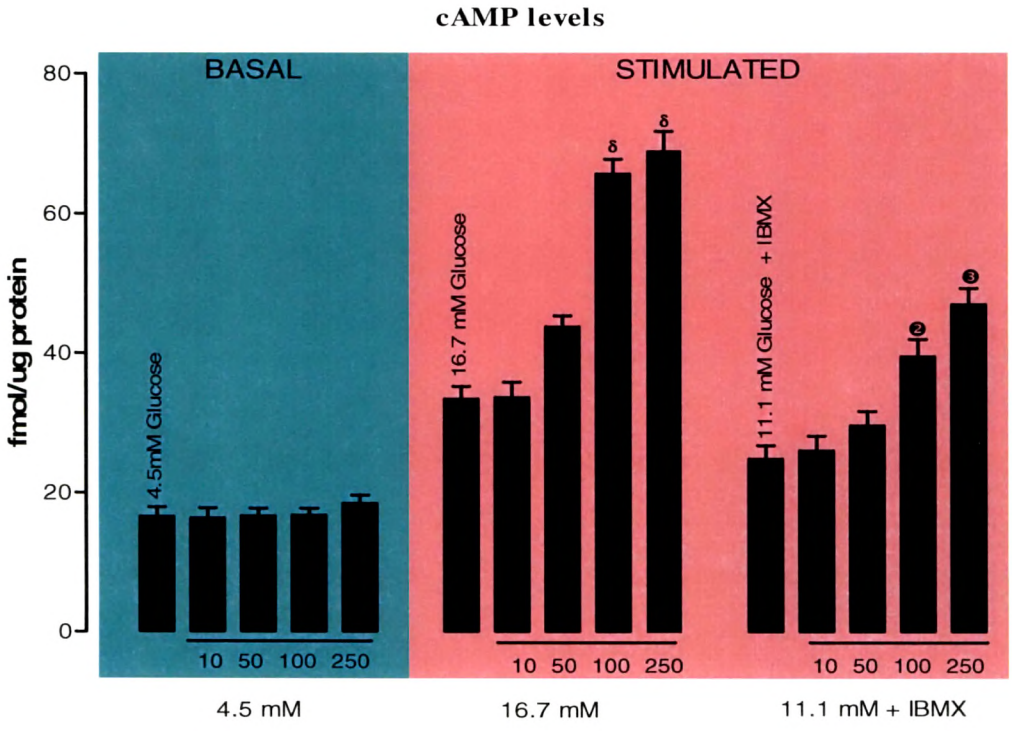

α = p <0.05, β = p <0.01, δ = p <0.001: 16.7mMglucose was compared to its 10,50,100,250
❶ = p <0.05, ❷ = p <0.01, ❸ = p <0.001: 11.1 mMglucose +IBMX was compared to its 10,50,100,250

Fig. 10: Effect of FRF on intracellular calcium levels in mouse islets

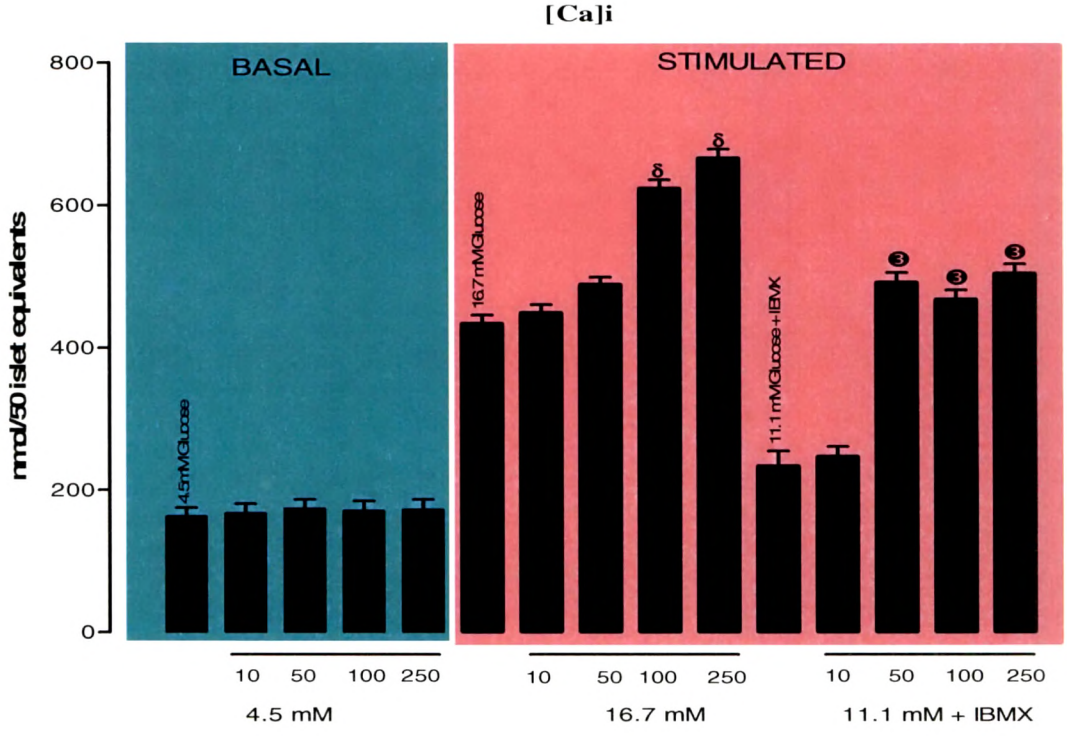

α = p <0.05, β = p <0.01, δ = p <0.001: 16.7mMglucose was compared to its 10,50,100,250
❶ = p <0.05, ❷ = p <0.01, ❸= p <0.001: 11.1 mMglucose +IBMX was compared to its 10,50,100,250

Fig. 11: Effect of FRF on MTT activity in mouse islets

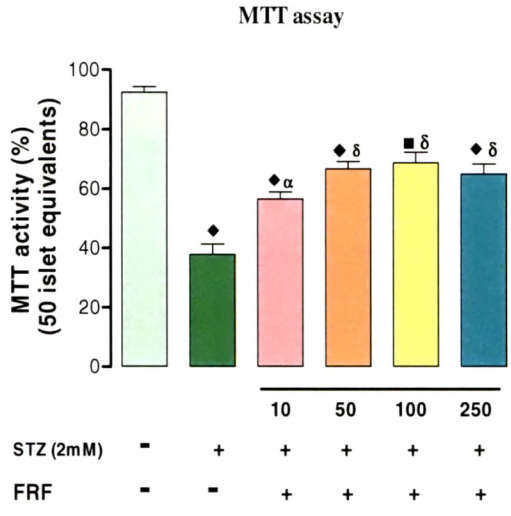

●=p<0.01, ■=p<0.001, ◆=p<0.0001: Control was compared with rest of the groups
α=p<0.01, β=p<0.001, δ=p<0.0001: Diabetic was compared with rest of the groups

Fig. 12: Effect of FRF on intracellular ROS activity in mouse islets

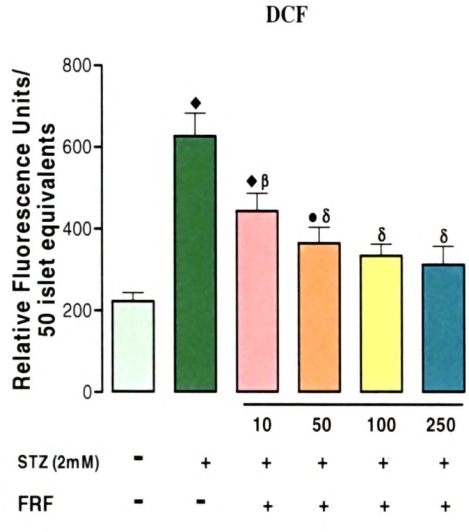

●=p<0.01, ■=p<0.001, ◆=p<0.0001: Control was compared with rest of the groups
α=p<0.01, β=p<0.001, δ=p<0.0001: Diabetic was compared with rest of the groups

Fig. 13: Effect of FRF on peroxynitrite activity in mouse islets

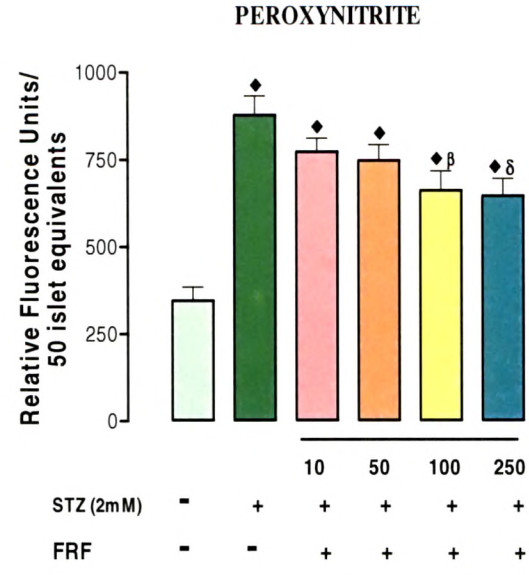

●=p<0.01, ■=p<0.001, ◆=p<0.0001: Control was compared with rest of the groups
α=p<0.01, β=p<0.001, δ=p<0.0001: Diabetic was compared with rest of the groups

Fig. 14: Effect of FRF on NO levels in mouse islets

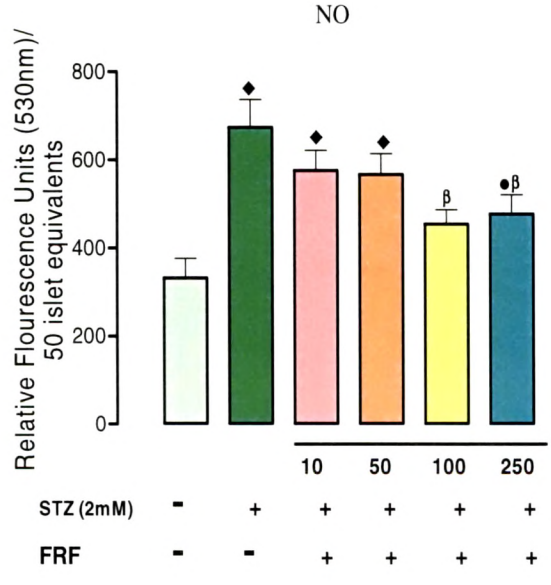

●=p<0.01, ■=p<0.001, ◆=p<0.0001: Control was compared with rest of the groups
α=p<0.01, β=p<0.001, δ=p<0.0001: Diabetic was compared with rest of the groups

Fig. 15: Effect of FRF on Mitochondrial membrane potential activity in mouse islets

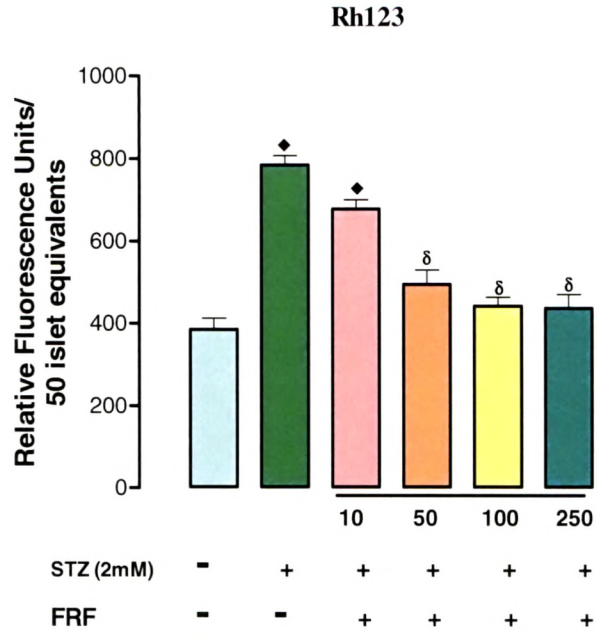

●=p<0.01, ■=p<0.001, ◆=p<0.0001: Control was compared with rest of the groups
α=p<0.01, β=p<0.001, δ=p<0.0001: Diabetic was compared with rest of the groups

Fig. 16: Effect of FRF on lipid peroxidation levels in mouse islets

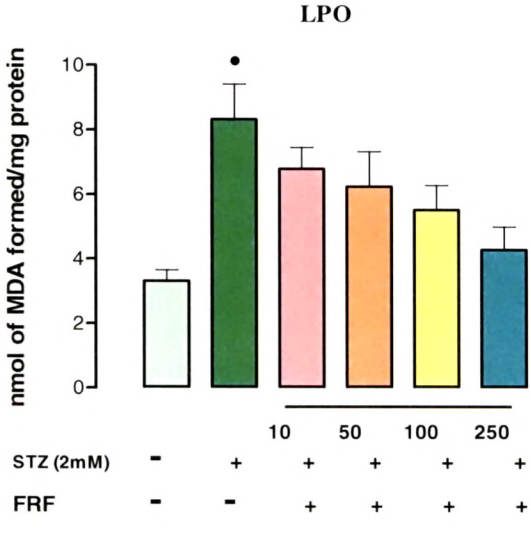

●=p<0.01, ■=p<0.001, ◆=p<0.0001: Control was compared with rest of the groups
α=p<0.01, β=p<0.001, δ=p<0.0001: Diabetic was compared with rest of the groups

Fig. 17: Effect of FRF on plasma glucose levels in mSTZ mice

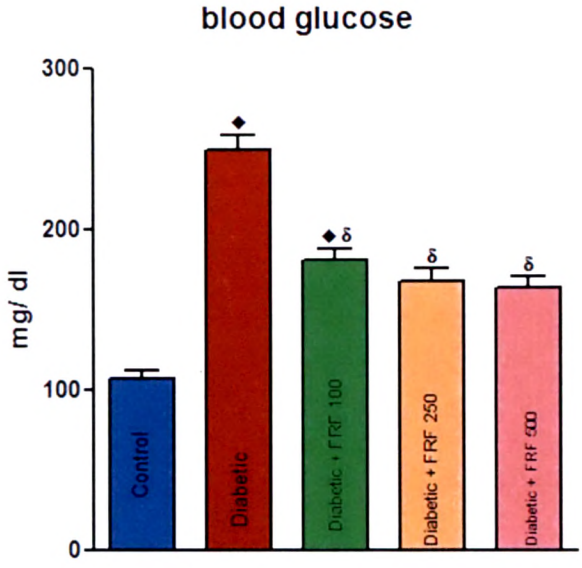

● = p < 0.05, ■=p <0.01, ◆=p < 0.001 sham was compared to other experimental groups
α = p <0.05, β = p <0.01, δ = p <0.001 Px day 7 was compared to Px day 7 + OI

Fig. 18:Effect of FRF on plasma insulin titre on mSTZ mice

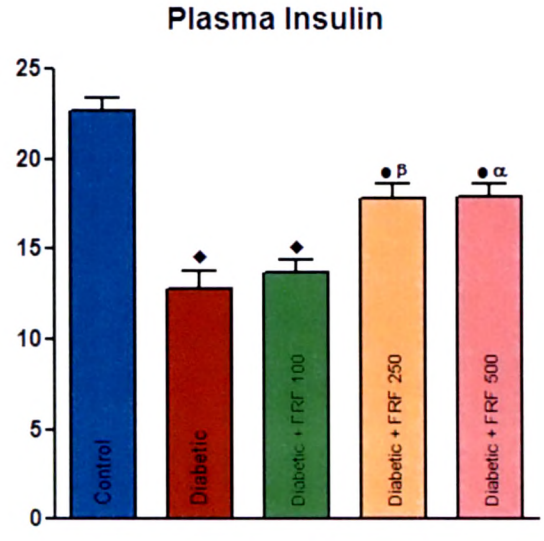

● = p < 0.05, ■=p <0.01, ◆=p < 0.001 sham was compared to other experimental groups
α = p <0.05, β = p <0.01, δ = p <0.001 Px day 7 was compared to Px day 7 + OI

Plate 1

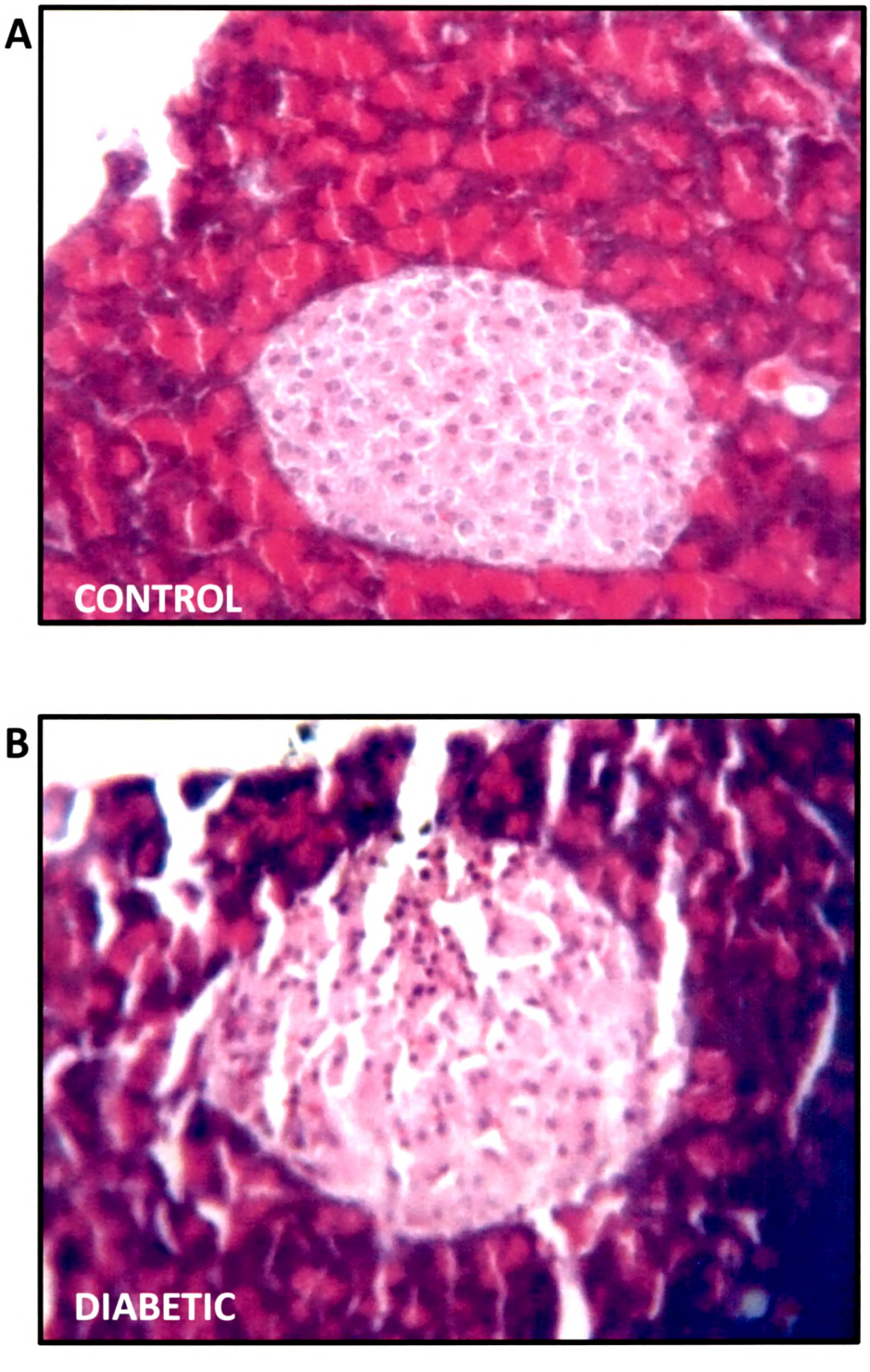

Plate 2

C

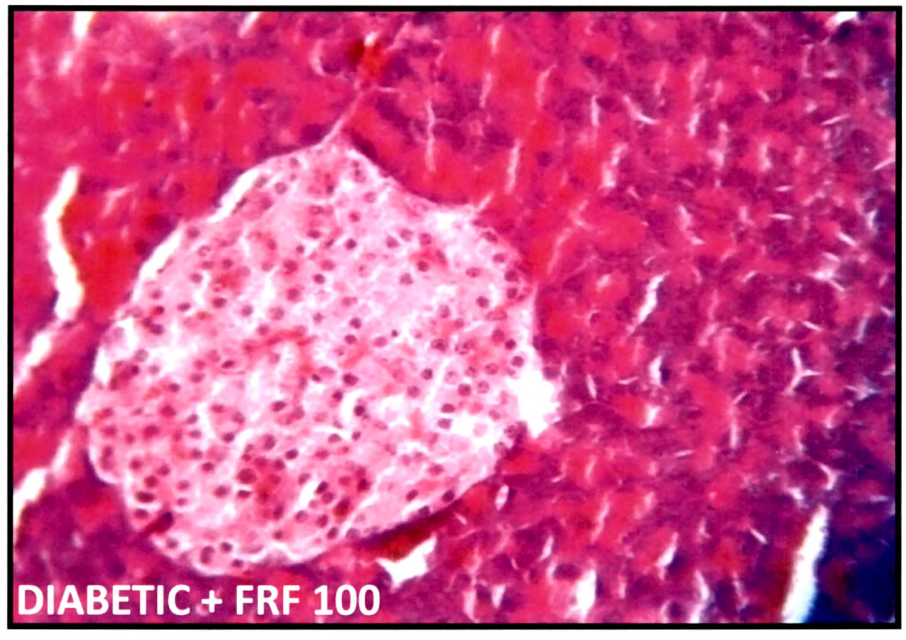

D

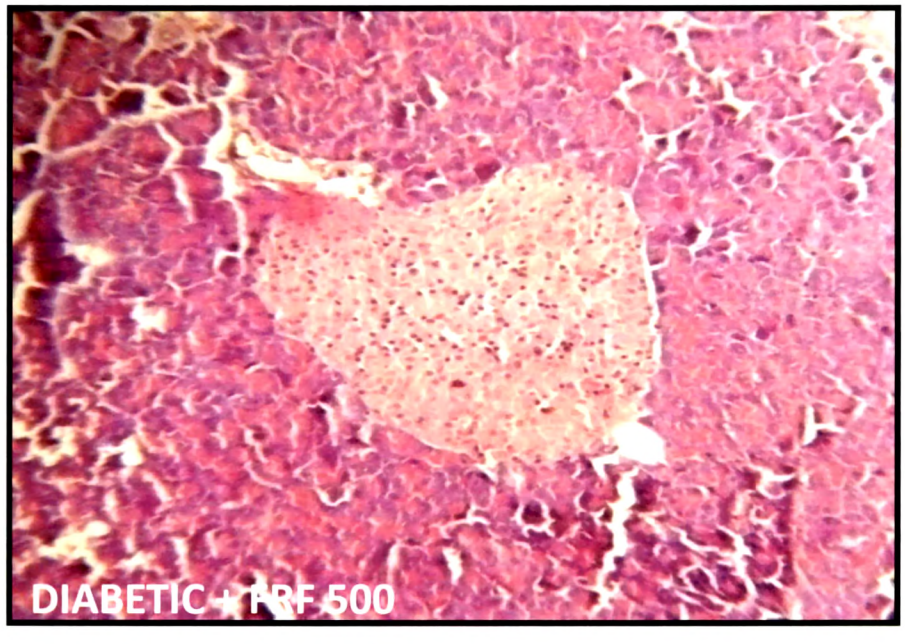

Plate 3

E

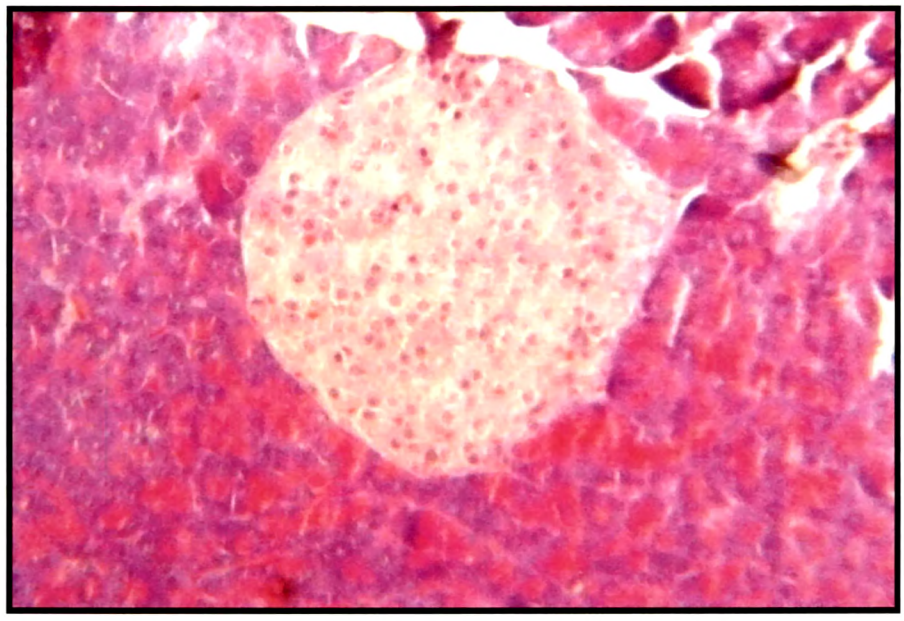

Images represent haemetoxylin and eosin stained sections of pancreas of A) Control animals showing intact islet histoarchitecture, B) Diabetic animals depicting islet cell destruction due to streptozotocin damage with wider intracellular spaces, C) Diabetic + FRF treated animals represent ameliorating effect of FRF, D) Diabetic + FRF250 and E) Diabetic + FRF 500 treated animals demonstrate improved islet integrity and morphology. Magnification 200X

Plate 4

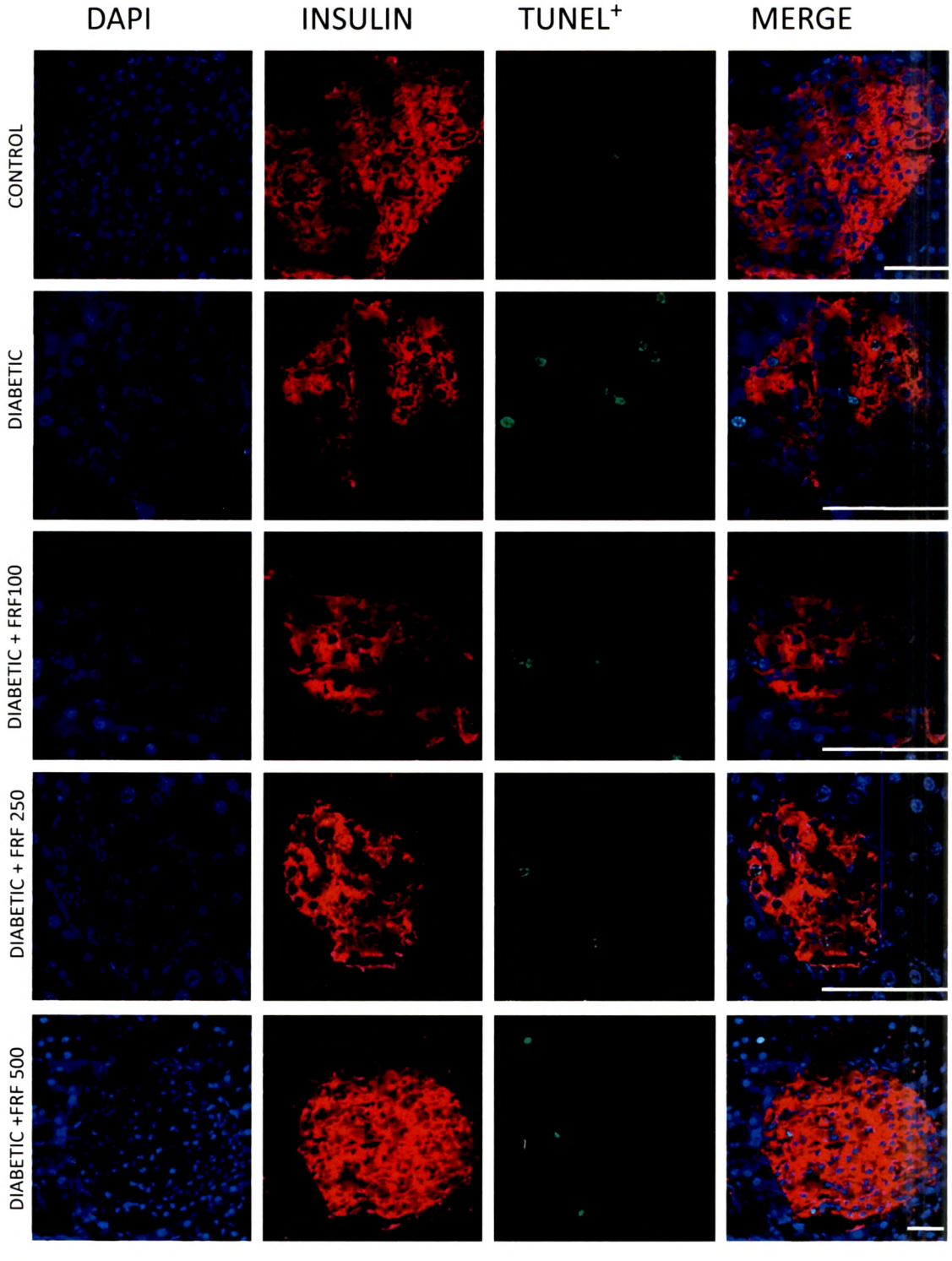

Images represent immunostained section of pancreas of A) Control, B) Diabetic, C) Diabetic + OI 100, D) Diabetic + OI 250 and E) Diabetic + OI 500. Guinea Pig anti insulin (red) and ApoBrdu-dUTP (green) were used as primary antibodies while TRITC and FITC as secondaries . DAPI (Blue) was used to visualize nuclei. The slides were visualized by Laser Scanning Confocal Microscope (LSM 510 META, ZEISS, Germany). Scale bar represents 100 µm.

Fig. 19: Effect of FRF on streptozotocin induced apoptosis.

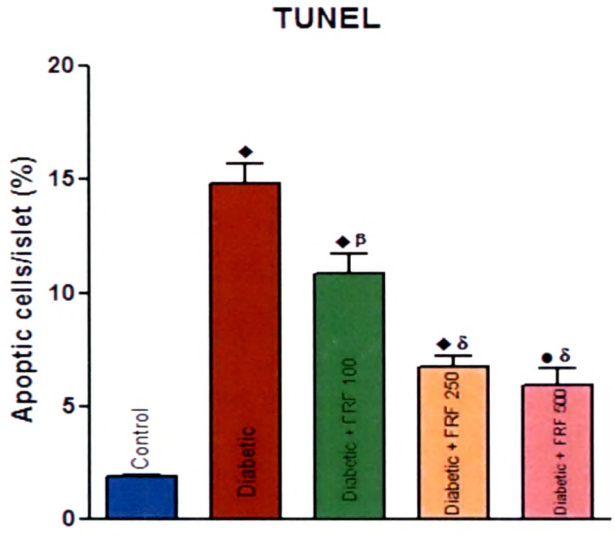

● = p < 0.05, ■=p <0.01, ◆=p < 0.001 sham was compared to other experimental groups
α = p <0.05, β = p <0.01, δ = p <0.001 Px day 7 was compared to Px day 7 + OI

PLATE 5: ISLET MORPHOLOGY AND SPECIFICITY

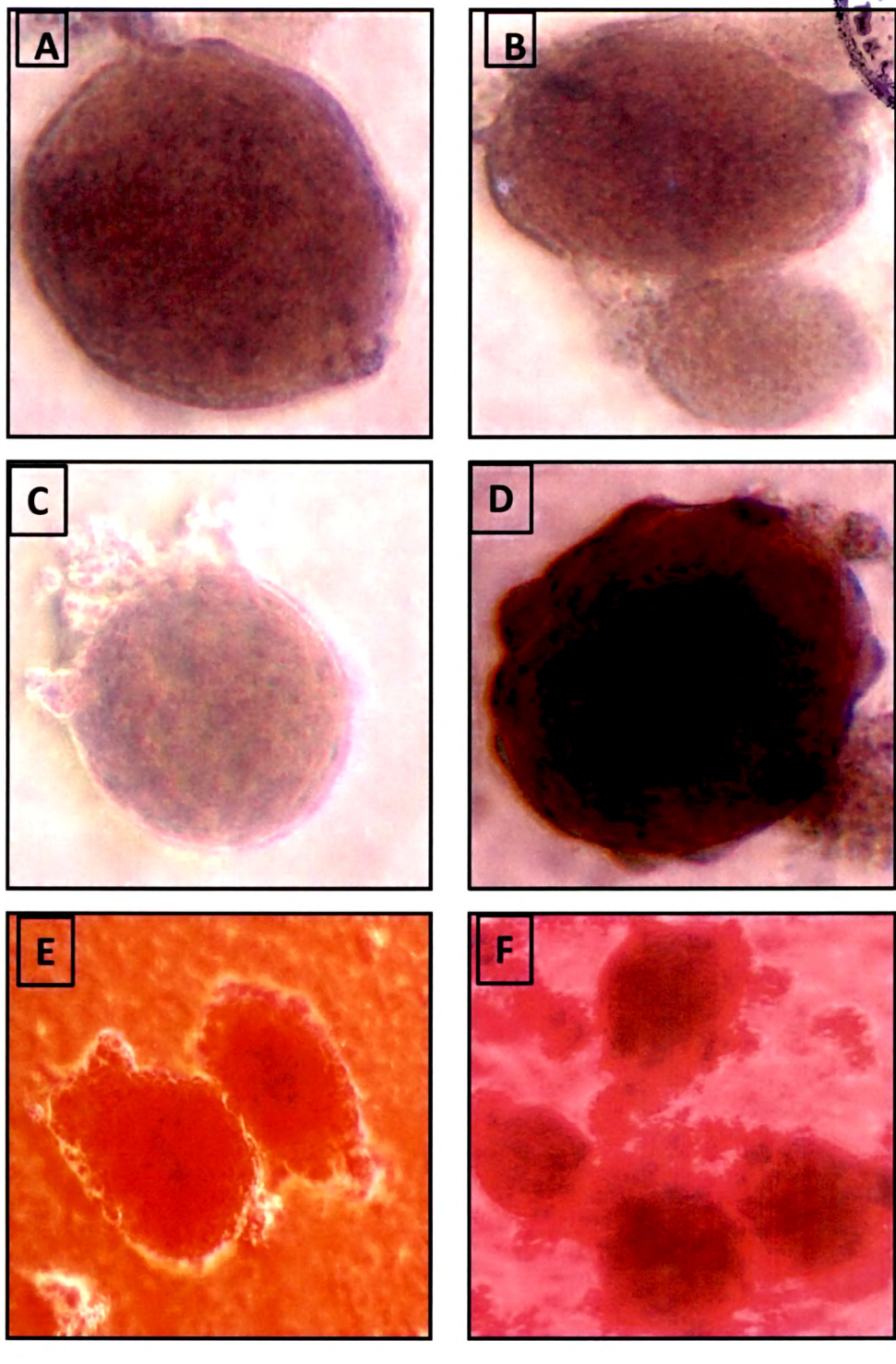

Images represent isolated pancreatic islets from BALB/c mice demonstrating functional islet morphology (A-C) and dead islets (D) . Islet specificity was assessed using dithizone staining (E,F)

Discussion:

Phytochemicals: Diabetic therapies in vogue currently are various oral anti-diabetic agents like sulfonylureas, biguanides, α-glucosidase inhibitors, and mostly used as mono-therapies or as combination therapies. Despite the availability of these drugs, diabetic management, sans side effects, is still a challenging proposition (Saxena and Kishore, 2004). It is in this context, botanicals have attracted greater attention world over in the use of complementary and alternative medicine, essentially due to their lesser known side effects compared to modern medicine (Hu *et al.,* 2003). Many traditional herbal remedies are in vogue for diabetes though, most of them remain in the realm of hidden wealth or folklore medication. Very few of the traditional plants have received scientific or medical attention. In recent times, two reviews have appeared on the chemistry of medicinal plants with anti-diabetic properties (Shapiro and Gong, 2003; Li *et al.*, 2004). There are many phytochemicals, which are non-nutritive plant chemicals, that have protective and / or disease preventive properties. Though produced essentially for their protection, many of these phytomolecules have shown up as remedies for human diseases. The introduction of these chemicals into modern alternative therapy awaits searching pharmacological testing and, such studies might provide a chestful of natural repertoire for diabetologist's pharmacy.

In the present study, preliminary phytochemical screening of OI leaves shows the presence of phenols, saponins, tannins, terpenoids, sterols and carbohydrates with negative indication for alkaloids, anthroquinones and amino acids. On a percentage basis, saponins, flavonoids, phenols and tannins seem to be the richest.

Literature is replete with reports of pharmacological properties of plant secondary metabolites. While alkaloids have been credited with anti-cancer and anti-

viral properties, saponins have been branded as cardiotomics and, flavonoids as anti-inflammatory moieties (Evans and Trease, 2002). Cushine and Lamb (2005) have shown flavonoids to be effective against cancer, inflammation and allergies. At the same time, alkaloids are related with anti-cancer, anti-diabetic, antiageing and anti-viral activities (Evans and Trease, 2002) and, tannins, with anti-diabetic, anti-diarrhoea, anti-sore throat, anti-skin ulcer and anti-dysentery properties (Okhale *et al.,* 2010). Saponins, terpenoids, flavonoids, tannins, sterols and alkaloids have all been attributed anti-inflammatory effects (Monach *et al.*, 1996; Latha *et al.,* 1998; Liu *et al.,* 2003; Akindele and Adeyemi, 2007; Orhan *et al.,* 2007). Similarly, glycosides, flavonoids, tannins and alkaloids have been shown to manifest hypoglycaemic activity (Oliver, 1980; Cherian and Augusti, 1995). Hypocholesteromic and anti-diabetic properties for saponins and blood sugar lowering ability for terpenoids have also been reported (Luo *et al.,* 1999; Rupasurighe *et al.,* 2003). Again, steroids and triterpenoids have been associated with analgesic properties while, steroids and saponins have been shown to influence activities of central nervous system (Sayyadh *et al.,* 2004; Argal and Pathak, 2006; Malanrajan *et al.,* 2006).

Our qualitative phytochemical screening reveals the presence of saponins, flavonoids, phenols and tannins as major constituents and all of them have shown different anti-diabetic properties (Burguires *et al.,* 2009; Tap *et al.,* 2009; Patra and Chua, 2010; Yang *et al.,* 2010). The earlier documented effects of whole aqueous or methanolic extract on various facets of diabetic manifestation lend credence to above reports (Chapter 1-3 & 5). Detailed analysis of methanolic and other extracts clearly reveal the presence of some interesting terpenes/steroids (β-sitosterol, hentriacontane, hentriacontanol acetate) and flavonoids (rutin, quercetin, keampherol, hesperidin, naringin).

Bioactivity:

The various extracts tested for their GSIS from RINm5F cells clearly show stimulatory effects for only ethanolic and methanolic extracts under basal glucose concentration of 4.5mM. Both these extracts show augmented GSIS under a stimulating glucose concentration of 16.7mM glucose with the effect of methanolic extract being maximal. However, 100 μg/ml butanol fraction also shows a significant GSIS. Apparently, active phytochemical ingredients with insulin secretogogue properties seem to be present in alcoholic extracts of OI, suggesting the nature of the secretogogues to be polar. The herein informed importance of polar compounds extractable in alcoholic solvents in inducing GSIS is supported by recent studies of alcoholic extracts of many plants showing potential for glucose stimulated insulin secretion from cell lines (Hoa *et al.*, 2004; Hannan *et al.*, 2007). Some of the active polar compounds also seem to possess insulinomimetic action as seen by the alcoholic extracts to promote glucose uptake in C2C12 Cells. Though these fractions promoted glucose uptake, it however was relatively lesser in comparison to insulin. Even in presence of insulin, though hexane, ethanolic and butanol fractions showed enhanced glucose uptake more than that seen without insulin, was nevertheless still lesser than insulin. However, methanolic fraction shows a complementary effect with insulin as, both doses of the extract promoted greater glucose uptake than insulin alone. Apparently, our methanolic extract has the active principle(s) that promote(s) glucose transport in larger concentration than in other fractions. The possible reason for the observed attenuation of glucose uptake (transport) promoting activity of the alcoholic extracts compared to insulin could be the presence of other interfering substances in the crude extracts that reduce the potential of the promoting molecules. Presence of phytochemicals in alcoholic extracts of other plants which promote glucose uptake in

muscle and adipose cell lines, is substantiated by our observed effect (Anadharajan *et al.*, 2006; Arayne *et al.*, 2007; Ravi *et al.*, 2009).

Based on our observations of methanolic fraction being more active in terms of insulin secretogogue and insulinomimetic functions and, richer flavonoid content in the mathanolic fraction, the isolated FRF was tested for its GSIS and glucose uptake properties. The observations made on RIN m5F and C2C12 cell lines clearly establish the very potent ability for eliciting insulin release and glucose uptake. The very high potency of our FRF fraction for glucoregulation is indicated by the dose dependent tremendously high insulin secretogogue expression (46% to 86% under basal glucose concentration and 11% to 37% under stimulating glucose concentration) and insulinomimetic role in glucose uptake (83% to 240% in the absence of insulin and 250% to 1450% in presence of insulin). Relatively, promotion of glucose uptake seems to be the more significant potential of FRF than, elicitation of insulin release. The observed markedly high potentials of FRF can be related with the identified mixture of flavonoids functioning together, either in an additive or synergistic fashion. Though there are reports of flavonoids promoting insulin secretion and glucose uptake under *in vitro* conditions (Hii and Howell, 1985; Jorge *et al.*, 2004; Pinent *et al.*, 2008; Qa dan *et al.*, 2009; Rao *et al.*, 2009), our FRF seems to exert relatively more powerful effects. The *in vitro* effect of FRF on insulin secretion seen in cell lines stands confirmed by the observed dose dependent increment by 23% under basal and by 44% under stimulated conditions of insulin release from isolated whole mouse islets. Clearly, the FRF mixture of OI has appreciable insulin secretogogue ability and is ideal for treatment of insulin deficiency under diabetic state.

The mechanism of glucose induced insulin secretion and other insulinotropic augmentors acting along with glucose, bring about ATP mediated closure of membrane K^+ channels and consequent depolarization leading to opening of Ca^{++} channels and intra-cellular elevation in Ca^{++} that mediate insulin secretory vesicle exocytosis. Most of the insulinotropic agents or potentiators function in a back ground of glucose stimulated permissive environment and stimulate adenylate cyclase mediated cAMP production and PLC-β mediated formation IP3 and DAG resulting in intracellular Ca^{++} signalling that culminate in PKA and PKC activation, which could in turn phosphorylate and again activate K_{ATP} channels. Elevation of these second messengers can also enhance insulin gene transcription (Kang *et al.,* 2001; Kashima *et al.,* 2001; Lawrence *et al.,* 2002; Doyle and Egan, 2003; Holz, 2004;). Even other pathways of insulin release independent of exocytosis but a release by altered membrane permeability are reported (Persand *et al.,* 1999; Bacova *et al.,* 2005; Ren *et al.,* 2007). Presently, the FRF fraction elevated the intra islet levels of both cAMP and Ca^{++} in a dose dependent manner in presence of stimulating concentration of glucose. The dose dependent increase in cAMP is manifested even in presence of IBMX, the PDE inhibitor. All the three doses of FRF equally high Ca^{++} level in presence of IBMX. It would appear from the present observations that, our FRF has potent ability to function as a potentiating insulinotropic agent for stimulating cAMP and Ca^{++} mediated insulin secretion under the permissive influence of glucose. It is also likely that, the potentiating insulin secretogogue action of FRF could also be mediated through GLP-1 action as, flavonoids are known to increase GLP-1 level as well as inhibit dipeptidyl peptidase IV (DPP-IV), the enzyme that metabolises GLP-1, both of which can efficiently upregulate insulin secretion from pancreatic islets in presence of glucose (Johnston *et al.*, 2002; Yogisha and Raveesha, 2010).

Exposure of islets to STZ shows significantly increased formation of peroxynitrite, NO and ROS with markedly elevated LPO and reduced cell viability. Islets exposed to STZ also show significantly increased mitochondrial membrane potential. Apparently, STZ causes severe oxidative and cytotoxic stress to islets likely to compromise their insulin releasing capacity. Presence of FRF in the medium along with STZ has depicted a dose dependent reversal of all the cytotoxic manifestations, with the highest dose of 250μg/ml normalising most of the measured parameters except for peroxynitrite and NO formation and total cell viability, suggesting the need for a probably higher dose to completely nullify the NO and peroxynitrite generation potential of STZ. The herein observed anti-oxidant, anti-ROS and NOs generation potentials and maintenance of mitochondrial membrane potential find substantial support from the reported anti-oxidant potential of flavonoids (Coskun *et al.,* 2005; Esmaeili *et al.*, 2009; Abdelmoaty *et al.,* 2010).

Validation of observed *in vitro* effects of FRF in multidose STZ mice has provided strong supportive evidence as, FRF has shown a dose dependent decrease in blood glucose level and increase in plasma insulin titre. Cytoprotective effect of FRF is also well evidenced by the histological appearance of islets from STZ+FRF mice compared to STZ mice. Further proof for the cytoprotective effect of FRF is provided by its anti-apoptotic potential as seen from the TUNEL assay and the noticeable insulin immunoreactivity. Many medicinal plants have been shown to have significant antidiabetic effects suggesting the presence of active phytochemicals (Kumar *et al.,* 2009; Sachan *et al.,* 2009; Vianna *et al.*, 2009; Ahad *et al.,* 2010).

Overall, the present investigation has shown the presence of active phytochemicals in the methanolic extract of OI and a rich mix of flavonoids. Moreover, the flavonoid mixture has been shown to have significant insulin

secretogogue, insulinomimetic and cytoprotective effects, as confirmed through the *in vitro* and *in vivo* models of evaluation.